EDGEWOOD

CHEMICAL BIOLOGICAL CENTER

U.S. ARMY SOLDIER AND BIOLOGICAL CHEMICAL COMMAND

ECBC-CR-011

ADSORBENTS FOR PRESSURE SWING ADSORPTION REGENERATION

David T. Croft
David K. Friday
Jeffrey M. Campbell

GUILD ASSOCIATES, INC.
Baltimore, MD 21236

June 1999

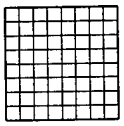

Guild
Associates, Inc.

Aberdeen Proving Ground, MD 21010-5424

Disclaimer

The findings in this report are not to be construed as an official Department of the Army position unless so designated by other authorizing documents.

REPORT DOCUMENTATION PAGE

Form Approved
OMB No. 0704-0188

1. AGENCY USE ONLY *(Leave Blank)*	2. REPORT DATE	3. REPORT TYPE AND DATES COVERED
	1999 June	Final; 98 Jan - 99 Mar

4. TITLE AND SUBTITLE
Adsorbents for Pressure Swing Adsorption Regeneration

5. FUNDING NUMBERS
C-DAAM01-96-C-0043

6. AUTHOR(S)
Croft, David T., Friday, David K., and Campbell, Jeffrey M.

7. PERFORMING ORGANIZATION NAME(S) AND ADDRESS(ES)
Guild Associates, Inc., 5022 Campbell Boulevard, Baltimore, MD 21236

8. PERFORMING ORGANIZATION REPORT NUMBER
ECBC-CR-011

9. SPONSORING/MONITORING AGENCY NAME(S) AND ADDRESS(ES)
DIR, ECBC*, ATTN: AMSSB-RRT-PF, APG, MD 21010-5424

10. SPONSORING/MONITORING AGENCY REPORT NUMBER

11. SUPPLEMENTARY NOTES
COR: David E. Tevault, AMSSB-RRT-PF, (410) 436-3860
*When this work started, the U.S. Army Edgewood Chemical and Biological Center (ECBC) was known as the U.S. Army Edgewood Research, Development and Engineering Center (ERDEC).

12a. DISTRIBUTION/AVAILABILITY STATEMENT
Approved for public release; distribution is unlimited.

12b. DISTRIBUTION CODE

13. ABSTRACT *(Maximum 200 words)*

This work is a continuation of the effort described in "Evaluation of Adsorbents for Pressure Swing Adsorption" (ERDEC-CR-260). Two significant modifications to the experimental apparatus described in the previous report have been made. A back-pressure regulator has been added to control chemical equilibrator pressure, thus making the feed concentration independent of downstream pressure. A discrete sampling capability has been developed that both confirms continuous concentration measurements and identifies possible chemical reaction products. Based on the results of ERDEC-CR-260, several different types of adsorbents were selected for further analysis. From these experiments, it was determined that the best performing adsorbents were silica gels. Experiments were then conducted using Silica Gel 40, Silica Gel 70A, Silica Gel 250A, and Silica Gel 500A to determine the affect of particle size and pore diameter on regeneration rate. Particle size effects were examined using two different mesh cuts of Silica Gel 40, and results clearly indicate that using smaller particles dramatically increases regeneration rates. All four silica gel samples were used to conduct the pore diameter study. A definite, near linear, relationship was found between pore size and clean-up rate. For example, the clean-up rate for Silica Gel 500A was twice that for Silica Gel 250A. The major conclusion drawn from this work is that the larger pore diameter silica gel adsorbents (250A and 500A) are the best materials for the feed-end layer in a PSA bed.

14. SUBJECT TERMS
Pressure swing adsorption
Adsorbent regeneration
Adsorbent screening

15. NUMBER OF PAGES
67

16. PRICE CODE

17. SECURITY CLASSIFICATION OF REPORT	18. SECURITY CLASSIFICATION OF THIS PAGE	19. SECURITY CLASSIFICATION OF ABSTRACT	20. LIMITATION OF ABSTRACT
UNCLASSIFIED	UNCLASSIFIED	UNCLASSIFIED	UL

Blank

PREFACE

The work described in this report was authorized under Contract No. DAAM01-96-C-0043. This work was started in January 1998 and completed in March 1999.

The use of either trade or manufacturers' names in this report does not constitute an official endorsement of any commercial products. This report may not be cited for purposes of advertisement.

This report has been approved for public release. Registered users should request additional copies from the Defense Technical Information Center; unregistered users should direct such requests to the National Technical Information Service.

Blank

CONTENTS

FIGURES

TABLES

ADSORBENTS FOR PRESSURE SWING ADSORPTION REGENERATION

1. INTRODUCTION

Pressure swing adsorption (PSA) plays an important role in many industrial processes, as well as military processes. One advantage PSA has over thermal swing adsorption (TSA) is that system pressure can be changed much more rapidly than system temperature. This makes short cycle times (e.g., 20 seconds) possible. If the adsorbed toxic gas can be removed from the adsorbent during the purge step, then rapid cycling reduces the required amount of adsorbent needed to protect against a given challenge. PSA is commonly used in air separation and air drying, where components are weakly adsorbed, and the adsorbent is easily regenerated. In applications where challenge chemicals are strongly adsorbed (such as organo-phosphorous compounds on activated carbon), the PSA purge step is not sufficient to regenerate the adsorbent.

This work develops methods to evaluate adsorbents for use in PSA systems intended to remove strongly-adsorbed contaminants from air. The goal is to find an adsorbent that has sufficient capacity to remove the strongly-adsorbed feed challenges, yet can be easily regenerated using flow rates and temperatures of a typical PSA purge step. The approach developed here uses breakthrough experiments to assess capacity and adsorption/desorption experiments to assess regeneration rate. Separate experiments, including N_2 BET measurements and particle-size studies, are also conducted to determine the affect that adsorbent physical characteristics have on regeneration rate.

The first work to be discussed is the broad screening of adsorbents. This is followed by an investigation of a suspected chemical reaction occurring during a screening experiment; then the effects of adsorbent size and pore size distributions on desorption rate is examined. There are three appendices. Appendix A reports data measured for the adsorbent screening phase of the study. Appendix B reports data measured in an effort to understand the effects particle size and pore-size distributions have on desorption rate.

2. APPARATUS AND EXPERIMENTS

Shown in Figure 1 is the schematic for the apparatus used to measure the adsorption and desorption data. Shown in the top left of the figure is the system used to generate the desired feed concentration. Clean, dry, (dew point temperature < -40 °C) house air regulated by a mass flow controller (MFC) (Tylan, Model FC-260, 0-500 sccm) is passed through an equilibrator cell containing the challenge chemical as a liquid (2-hexanol). The diluent stream is also clean house air regulated by a MFC (Tylan, Model FC-260, 0-1000 sccm). There are two normally-closed, two-way valves (Valves 1 and 2, Skinner, B2D31175) at the inlet and outlet of the equilibrator cell that can isolate the cell, if required. More recent improvements to the

system include the pressure gauge and the back-pressure regulator. The challenge concentration is fixed by the sparger temperature, sparger pressure, and the ratio of the sparger and diluent flows. In order to maintain constant pressure (and therefore downstream concentration) in the sparger, the back pressure regulator is set to maintain a pressure greater than the maximum pressure drop due to downstream restrictions.

The purge air is clean, dry, house air regulated using a MFC (Tylan, Model FC-260, 0-1000 sccm). Three pneumatically actuated four-way valves (Valves 3, 4, and 5) (Whitey SS-43YF2-125) direct the flow path for various modes of operation. Valve 3 is used to select either the purge air stream or the feed air stream. Valve 4 is used to direct the flow stream to the adsorbent bed or bypass the bed directly to the vent. The adsorbent bed is a 0.635-cm stainless steel tube, 30 cm in length with 0.277 cm inside diameter, contained in a temperature-controlled jacket. Valve 5 determines the flow direction through the bed. The purge flow direction is counter-current to the challenge flow direction, so this valve must be changed when going from the challenge to the purge steps.

The sampling system is shown in Figure 2. As with the previous design,[1] the effluent concentration is continuously monitored using the flame ionization detector (FID) of a Perkin-Elmer Gas Chromatograph (GC). A fraction of the effluent stream is drawn through a Metal Bellows (MB-41) pump and directed to a GC oven. Within the oven, the sample stream is split. The majority of the flow is sent to the vent. The remaining sample flow is sent through a restrictor (a 4 cm length of .01 cm ID, 0.159 cm OD, tubing) directly to the FID. The metering valve on the vent line and the restrictor allows control of the flow rate to the detector. This arrangement keeps the lag time (as well as dispersion in the lines) to a minimum by allowing for flow rates on the order of 50 sccm through the lengthy sample line. Only about 6-10 sccm is fed to the detector, and the length of this tube section is minimized. Recent changes to the system include replacing the stainless tubing with an inert plastic (polyetheretherketone, PEEK) tubing upstream of the detectors (shown in diagram) and adding a discrete sampling capability. For discrete sampling, a separate fraction of the effluent stream is drawn by an additional MB41 pump and passed to a 6-port valve (Valco Instruments Co., Model E60). The valve rotor can assume two positions. In one, the effluent directed to the valve is directed through a sample loop, and pure carrier gas is directed through the GC column. In the other position (shown in Figure 2), carrier gas flushes the sample loop, directing a pulse of effluent through the GC column. The column outlet goes to a second FID.

---

[1] Campbell, Jeffrey M., Croft, David T., Friday, David K., Evaluation of Adsorbents for Pressure Swing Adsorption, ERDEC-CR-260, U.S. Army Edgewood Research, Development and Engineering Center, Aberdeen Proving Ground, MD, April 1998, UNCLASSIFIED Report.

3. PROCEDURE FOR ADSORPTION/DESORPTION EXPERIMENTS

3.1 Adsorbent Loading.

Adsorbent is weighed and placed into a tube with an inside diameter of 7.0 cm. A portion of the adsorbent sample is also placed in an oven overnight at 100 °C to determine the moisture content of the sample. The dry weight in the bed is calculated using the wet weight and moisture content.

3.2 Pretreatment.

The temperature of the adsorbent bed is raised to 150 °C and held at this temperature while purging with clean air until the detector response is below its limit, approximately 0.2 mV for the Perkin-Elmer AutoSystem GC. This corresponds to a concentration of about 0.15 ppm. The bed temperature is then set to 30 °C.

3.3 Calibration.

When the temperature of the adsorbent bed reaches 30 °C, the valves are switched so the challenge concentration of either 2,000 mg/m^3 or 4,000 mg/m^3 flows directly to the detector (bypasses the adsorbent bed). When the detector response remains constant based on an equilibration criterion, a calibration factor is calculated.

3.4 Detector Purge.

The valves are changed to allow clean purge air to flow directly to the detector, while the airstream containing the challenge concentration is vented. This continues until the detector response is below its detection limit.

3.5 Challenge.

Two challenge scenarios are used. For the 7,000 Ct ($mg*min/m^3$) challenge experiments, the valves are changed to direct the 2,000 mg/m^3 challenge concentration stream to flow over the bed for 3.5 minutes. For the 20,000-Ct challenge, 4,000 mg/m^3 is directed to the bed for 5 minutes. The challenge volumetric flow rate for all experiments is 0.70 SLPM (0 °C, 1atm), which corresponds to a superficial linear velocity of 37 cm/sec.

3.6 Desorption.

The valves are changed to shut off the sparger flow and to direct clean purge air through the adsorbent bed in the opposite direction of the challenge step. The bed temperature set point is changed to 50 °C, 100 °C or 150 °C, and the ramp rate is set to 2 °C/min. The desorption step continues until the bed temperature reaches its setpoint value, and the detector

response is below its detection limit. The desorption volumetric flow rate for all experiments is 0.91 SLPM, which corresponds to a superficial linear velocity of 49 cm/sec.

3.7 High Temperature Desorption.

The bed temperature is increased to 150 °C, with a ramp rate of 2 °C/min, and held at this temperature until the detector response is below its detection limit. This step is accomplished to close the mass balance, as well as to clean the bed for the following breakthrough experiment.

3.8 Breakthrough.

The adsorbent bed temperature is decreased to 30 °C. The valves are switched to direct the 2,000 mg/m^3 challenge concentration over the adsorbent bed. The system continues to challenge the bed and analyze the effluent. When the effluent concentration reaches 1/2 the challenge concentration, the time is doubled, and this is the time at which the breakthrough step is stopped.

4. PRELIMINARY SCREENING RESULTS

The first set of experiments was intended to determine the regeneration characteristics of six adsorbents. These include Silica Gel 250A (Grace-Davidson), Sorbead RF (Solvay Chemicals), Activated Alumina (Grace-Davidson), Calcined Sorbead RF(calcined by Guild Associates, Inc.), Zirconia XZ 16122 (Norton Chemical Process Corp.), and Zirconia 16154 (Norton Chemical Process Corp). Dates of the experiments, challenge chemicals, and other information are given in Table 1. The challenge chemicals were 2-hexanol (Aldrich, 99%, CAS# 626-93-7), and 1,1,1-trifluoroethane (DuPont, HCFC-123, CAS# 306-83-2). The vapor pressure parameters used to calculate the feed concentrations are given in Table 2.

4.1 Purge Step and Desorption Rate.

To better understand the nature of the experiments conducted and to explain what the entries in Table 1 mean, the desorption step of Experiment 7 is treated in detail. These results are shown in Figure 3. Both Table 1 and Figure 3 will be used in the following discussion. The column labeled Desorption T is the target desorption temperature. The desorption step actually starts at 30 °C. When the effluent concentration drops below a threshold concentration, the adsorbent temperature is ramped up to the target desorption temperature. The column labeled Mass Bal (%) is equal to 100 x mass of chemical recovered divided by the mass of chemical challenged. The mass of chemical recovered is obtained by integrating the effluent concentration curve for the entire desorption step, including the high temperature purge (Step 6 in the procedure) at the end of every desorption step. This value should be near 100%. Values that are not near 100% indicate that either the adsorbate is too strongly bound to be removed, chemical reaction is occurring, or that the chemical calibration is not correct. Figure 3 shows vapor-phase concentrations, temperatures, and the integrated material balance versus time. The

Table 1. Summary of Adsorption/Desorption Experiments.

Exp. No.	Date	Adsorbent	Adsorbate	Challenge Ct ($mg*min/m^3$)	Desorp. T (°C)	Mass Bal. (%)	Peak Conc. (ppm)	2nd peak Conc. (ppm)	T at 2nd Peak (°C)
1	4/8/98	Silica Gel 250Å	2-hexanol	7,000	50	96.0	44.8	6.5	48.0
2	4/9/98	Silica Gel 250Å	2-hexanol	7,000	100	98.3	37.0	64.9	94.5
3	4/10/98	Silica Gel 250Å	2-hexanol	7,000	150	78.3	144.7	56.7	93.0
4	4/11/98	Silica Gel 250Å	2-hexanol	7,000	50	99.2	39.7	67.6	48.0
5	4/13/98	Sorbead RF	2-hexanol	7,000	50	105.0	41.6	6.7	51.3
6	4/14/98	Sorbead RF	2-hexanol	7,000	100	135.7	45.2	125.5	95.0
7	4/22/98	Sorbead RF	2-hexanol	7,000	100	103.0	44.0	69.3	90.4
8	4/23/98	Sorbead RF	2-hexanol	7,000	150	98.4	47.2	166.4	110.8
9	4/24/98	Alumina	2-hexanol	7,000	50	47.4	48.9	16.5	144.5
10	4/25/98	Alumina	2-hexanol	7,000	50	70.9	57.7	22.1	192.6
11	4/27/98	Alumina	2-hexanol	7,000	50	55.3	60.7	63.8	202.3
12	4/28/98	Silica Gel 250Å	2-hexanol	7,000	50	96.1	93.5	21.4	47.3
13	4/29/98	Silica Gel 250Å	2-hexanol	7,000	100	101.0	91.2	114.4	76.3
14	4/30/98	Silica Gel 250Å	2-hexanol	7,000	150	100.6	91.3	143.3	83.0
15	5/5/98	Alumina	2-hexanol	7,000	100	88.6	44.2	11.1	83.0
16	5/6/98	Silica Gel 250Å	2-hexanol	20,000	50	97.4	231.7	75.6	50.2
17	5/7/98	Silica Gel 250Å	2-hexanol	20,000	100	96.9	232.5	283.1	82.3
18	5/8/98	Silica Gel 250Å	2-hexanol	20,000	150	96.5	229.5	397.8	94.1
19	5/9b/98	Sorbead RF	2-hexanol	20,000	100	95.3	57.3	190.7	104.8
20	5/9/98	Sorbead RF	2-hexanol	20,000	50	90.6	56.2	11.7	57.6
21	5/10/98	Sorbead RF	2-hexanol	20,000	150	92.6	57.4	580.8	130.4
22	5/11/98	Calcined Sorbead RF	2-hexanol	20,000	100	92.7	76.1	130.4	102.3
23	5/13/98	Zirconia (XZ 16122)	2-hexanol	20,000	100	30.1	187.5	7.3	70.4
24	5/15/98	Zirconia (XZ 16154)	2-hexanol	20,000	100	14.9	106.4	4.4	74.8
25	5/18/98	Silica Gel 250Å	2-hexanol	20,000	100	105.9	363.9	270.7	79.8
26	5/19/98	Silica Gel 250Å	2-hexanol	20,000	100	96.4	597.2	256.2	80.6
27	5/27/98	Sorbead RF	HCFC-123	20,000	50	42.0	484.8	none	none
28	5/28/98	Silica Gel 250Å	HCFC-123	20,000	50	32.4	587.2	none	none
29	5/29/98	Silica Gel 250Å	HCFC-123	4,000	50	11.1	30.5	none	none
30	6/1/98	Alumina	HCFC-123	20,000	50	69.9	415.0	none	none
31	6/2/98	Alumina	HCFC-123	20,000	50	71.5	417.9	none	none

zero on the time axis corresponds to the beginning of the purge step (immediately following the challenge step).

Table 2. Antoine Vapor Pressure Constant (*P* in Pa, *T* in K).

	A	B	C
2-Hexanol	21.61	3159.0	-100.0
HCFC-123	21.20	2588	-33.5

The first concentration peak typically occurs in the first minute of the desorption step when the temperature setpoint is 30 °C. This value is a measure of how strongly adsorbed the chemical is at 30 °C. The height of the peak is related to the slope of the drop in concentration as purge begins. Adsorbents that are difficult to regenerate tend to have lower concentration first peaks, because the rate at which they give up adsorbate is low. This peak concentration at 30 °C is recorded under the heading Peak Conc. in Table 1. The second peak concentration occurs at about 25 minutes. This peak results from heating the adsorbent from 30 °C to 100 °C. The height of this peak is related to the enthalpy of adsorption, as well as mass transfer characteristics. The small, third peak at 200 minutes results when the temperature is raised to 150 °C to completely purge the adsorbent. This is Step 6 in the procedure.

4.2 Breakthrough Experiments and Adsorption Capacity.

Breakthrough experiments were performed for each adsorbent-adsorbate pair. This is Step 7 in the procedure. These data are also critical to understanding the behavior of these adsorbents, and their potential use in PSA systems.

The adsorption behavior of each adsorbent is summarized in Table 3. The time to 50% of C_{feed} is used to calculate the adsorption capacity. None of the adsorbents considered have a useful adsorption capacity for HCFC-123. Loadings in the 10^{-4} g/g range are an order of magnitude less than the loading of air at ambient conditions.

Another important aspect shown in Table 3 is given in the last column. The shape of the breakthrough is critical for use in a military purification system. The shape is labeled as "Fav" for favorable. This means that the isotherm is concave down, and it produces a standard "s-shaped" breakthrough curve. The label "Unfav" means the breakthrough curves show an immediate jump in concentration. This results from linear or unfavorably shaped (concave up) isotherm shape. This adsorption equilibria behavior, although it is good for desorption, would require another layer downstream to prevent low concentrations from reaching the product stream.

Table 3. Summary of the Breakthrough Experiments.

Exp. No.	Date	Adsorbent	Adsorbate	Cfeed (mg/m^3)	Time to 50% of Cfeed (min)	Dry Weight (g)	Loading (g/g)	Shape
6	4/14/98	Sorbead RF	2-Hexanol	2,000	239.33	0.9345	1.62E-01	Fav
10	4/25/98	Alumina	2-Hexanol	2,000	156.27	1.2478	1.05E-01	Fav
13	4/29/98	Silica Gel 250Å	2-Hexanol	2,000	101.52	0.9442	1.34E-01	Fav
22	5/11/98	Calcined Sorbead RF	2-Hexanol	2,000	360.98	1.069	2.53E-01	Fav
23	5/13/98	Zirconia (XZ 16122)	2-Hexanol	2,000	29.28	1.7534	1.26E-02	Unfav
24	5/15/98	Zirconia (XZ 16154)	2-Hexanol	2,000	184.72	2.0358	6.56E-02	Unfav
27	5/27/98	Sorbead RF	HCFC-123	4,000	0.1	1.1918	1.64E-04	Unfav
28	5/28/98	Silica Gel 250Å	HCFC-123	4,000	0.6	3.365	3.55E-04	Fav
30	6/1/98	Alumina	HCFC-123	4,000	0.85	7.5125	1.58E-04	Unfav

4.3 Discrete Sampling.

The preliminary screening experiments (Table 1) were conducted using the back pressure regulator, pressure gauge, and PEEK tubing, but without the discrete sampling capability. The discrete sampling system was added based on the results of the alumina and zirconia experiments. The mass balance was not closed in these experiments, and attempts were made to determine the reason(s). The experimental procedure was modified for several alumina experiments. The first change was to increase the final desorption temperature (Step 6 in the procedure) to above 150 °C. For Experiment 9, the mass balance was 47.43% when the final purge temperature was 150 °C. For Experiment 10, the final purge temperature was increased to 200 °C hoping to achieve a mass balance. The mass balance improved to 70.9%. The final purge temperature was then increased to 250 °C for Experiment 11. However, the mass balance went down to 55.3%. A decreasing mass balance with increasing temperature is a clear indication that chemical reactions are occurring with the 2-hexanol. Further, since we are using an FID, the products of the chemical reaction must be less sensitive than 2-hexanol; or they are very strongly adsorbed. The second change was a modification to the apparatus.

Experiment 32 (Figure 4) is an alumina experiment conducted with apparatus capable of discrete, as well as continuous sampling. The feed challenge was a 7,000 Ct at 2,000 mg/m3 of 2-Hexanol. During the purge step, the temperature was first raised to 50 °C and then finally to 150 °C. Most discrete sampling data points closely followed continuous sampling results as shown in Figure 4. There are some discrepancies during part of the desorption step though the last few discrete points coincide with the continuous measurement. Vapor-phase reaction products were not detected in the effluent by the GC. The material balance for the adsorption/desorption experiment was consistent with the previous result and was below 50%. Our conclusion is that 2-hexanol reacts on activated alumina.

5. SILICA GEL REGENERABILITY

The following experiments were conducted to determine the relationship between regeneration rate and the structural properties (pore size distribution) of a particular adsorbent. All experiments were conducted using silica gels. The first set of experiments examined the effect particle size has on regenerability.

5.1 Regeneration Rate vs. Particle Size.

It is well known that particle size affects mass transfer rates. Two experiments were conducted using 10x12 mesh and 18x25 mesh Silica Gel 40 under identical conditions. These experiments are listed in Table 4 (Experiments 33 and 34), and results of the desorption step are shown in Figure 5. Figure 5 shows the experiment using smaller particles (18x25 mesh) results in a first peak value between 35 and 40 ppm, while the experiment using the larger particles (10x12 mesh) results in a first peak concentration of about 5 ppm. Recall that the first peak height is related to the rate at which adsorbate is given up by the adsorbent. The second peak concentration of the smaller mesh silica gel is about 30% higher than the adsorbent with the larger mesh. This peak occurs as the adsorbent is heated to 50 °C; and in this case, because the enthalpy of adsorption is the same in each of the experiments, it is also related to the rate at which material can diffuse out of the adsorbent. These results show clearly that adsorbent regeneration rates are affected by particle size. They also show that smaller particles can provide a significant improvement in regeneration rate. Of course, smaller particles increase pressure drop through the bed, which in turn decreases purge efficiency and increases energy costs.

Table 4. 2-Hexanol Challenge of 2,000 mg/m^3 for 3.5 Minutes (7, 000 Ct).

Exp. No.	Date	Adsorbent	Mesh	a (cm^2/cm^3)	30 min. Desorption
33	11/18/98	Silica Gel 40	18x25	3.6	8.5%
34	11/20/98	Silica Gel 40	10x12	1.6	5%

A quantitative analysis of the silica gel 40 particle size experiments can be performed using the mass balance calculations shown in Figure 3. During the first 30 minutes of both experiments, the temperature of the adsorbent is maintained at a constant 30 °C. The rate at which the mass balance is closed during this time is shown in Figure 6. The rate of desorption from the 18x25 mesh particles is initially rapid and then approaches a constant rate (straight line). For the 10x12 mesh particles, much less comes off initially, and a constant rate is achieved earlier. The approximate external surface area per volume for the particles is listed in Table 4, along with the extent to which the mass balance was closed within the first 30 minutes of the experiment. As may be expected, the larger the mass transfer area per volume, the greater the desorption rate.

5.2 Regeneration Rate vs. Pore Size.

The following experiments (see Table 5) were conducted to determine the affect pore size has on desorption rate. Four silica gel adsorbents, each with a different average pore diameter, were tested using the same mesh size. Shown in Table 5 are the nominal average pore size, the time required for the concentration to reach 50% of the feed concentration during the breakthrough part of the experiment (proportional to the adsorption capacity at the feed concentration), the adsorbent sample mass dry, the final mass balance, and the average desorption rate during the first 20 minutes of the desorption step (at 30 °C). The nominal average pore size was taken from the name of the silica gel given to it by the manufacturer. For silica gel 250A and 500A, for example, the manufacturer claims the number is representative of the mean pore diameter in Angstrom units. Progress towards closure of the mass balance is shown in Figure 7. After 20 minutes, the mass balance for silica gel 500A was about 23.6 % closed. After 20 minutes, the mass balance of silica gel 250A is 12.3 % closed.

Regeneration rates for the four adsorbents are shown in Figure 7. These data are from the initial desorption step at 30 °C. There is a near linear relationship between the nominal mean pore size and the rate at which the mass balance is closed for all four silica gels. Plotted in Figure 8 are the relative adsorption capacity and the relative desorption rate for each adsorbent using the adsorption capacity and desorption rate of silica gel 250A as unity.

A comparison of each adsorbent with 250A shows an interesting result. The product of the relative capacity and the relative desorption rate for each silica gel is about 1. The largest deviation is for the silica gel 500A where the product is about 0.7. The product value is important because it relates the amount of adsorbent required to the clean-up rate.

Table 5. Experiments Conducted With Fresh Adsorbent Samples.

Exp. No.	Date	Silica Gel	50% Breakthrough	Mass (g)	Mass Balance	Purge Rate
35	1/19/99	500A	35 min	1.1	92.6 %	1.179 %/min
38	1/22/99	70	268 min	1.4	90.6 %	0.386 %/min
40	1/28/99	40	279 min	1. 5	90.1 %	0.174 %/min
43	2/8/99	250A	89 min	1.0	89.3 %	0.615 %/min

6. DISCUSSION

Referring to Table 1, the effect of the feed dose appears to be minimal. In general, the 20,000-Ct challenge shows peaks about twice as large as the 7,000-Ct challenge. This is because the feed concentration is twice as large in the 20,000-Ct challenge.

The particle size experiments conducted using silica gel confirm that particle size significantly affects regeneration rate. The 18x25 mesh particles (3.6 cm^2/cm^3) have slightly more than twice as much mass transfer area per unit volume than the 10x12 mesh particles (1.6 cm^2/cm^3). The amount of the challenge recovered in the first 30 minutes is almost twice as much using the smaller particles, 8.5% verses 5%. A plot of challenge recovery versus time (Figure 6) shows that about 4% of the 2-hexanol is recovered in the first 5 minutes in the 18x25 mesh case. Thus, roughly half of the 2-hexanol recovered in 30 minutes was recovered in the first 5 minutes. After about 5 minutes, the rate of recovery is almost independent of particle size since both the 18x25 and the 10x12 mesh recovery lines have almost the same slope. A straight-line approach towards closure of the mass balance implies a constant effluent concentration.

The pronounced curvature in Figure 6 for the smaller particles is due to a rapid change in the effluent concentration at the start of the purge step. Curvature does not appear for the larger particles because the drop is so rapid that it cannot be measured. The differences in the results for the two particle sizes are due to mass transfer effects in BOTH the challenge and purge steps. During the challenge step, chemical penetrates further into the bed when the larger particles are used. Therefore, the average loading on each particle is lower, and just as important, particles further down the bed have chemical adsorbed on them. This, in turn, results in lower adsorbed-phase concentrations at the bed outlet when the desorption step is started; thus, the effluent concentration is lower. During the purge step, the larger particles also exhibit the slower mass transfer rates. The combination of the slower rates during both challenge and desorption for the 10x12 mesh particles results in a lower concentration first peak.

The mass balance closure rates for the four silica gels tested (Figure 7) show the same general shape as the results in Figure 6. Each adsorbent is approximately the same mesh cut. It is interesting to note here that the desorption rate starts high and rapidly falls with time. Figure 8 indicates that the adsorption capacity increases with decreasing pore size while the desorption rate increases. The product of the relative adsorption capacity and the relative desorption rate is almost the same for each material, although Silica Gel 500A is the lowest at 0.7.

Based on the results presented here, Silica Gel 250Å is the probably best adsorbent of the ones tested for use in regenerable adsorption systems. It exhibits favorable adsorption equilibria, yet the heat of adsorption is low allowing for superior purge characteristics over the other adsorbents tested. Some of the improved performance is attributable to the small particle size. However, the breakthrough shape and the heat of adsorption (i.e., its behavior as the temperature is changed) are fundamental properties of the adsorbent. If adsorption capacity is not an issue, then Silica Gel 500A, with its superior desorption rates, would be a better choice. Since adsorbent was tested in the presence of high humidity, it is not clear how the humidity could affect the selection.

7. CONCLUSIONS

1. Silica Gel 250Å and Silica Gel 500Å are both good candidates for further study. They both have relatively rapid desorption rates, as well as reasonably good adsorption capacity.

2. Adsorbent mesh cut significantly affects the desorption rate. The desorption rate during the first 30 minutes of the desorption step was almost twice as fast for 18x25 mesh particles as it was for 10x12 mesh particles of the same adsorbent.

8. RECOMMENDATIONS

1. The choice of simulants for the nerve and blister agents needs to be better understood. Clearly, when considering non-carbon based adsorbents, there appear to be differences in the adsorption behavior that are not related to pore size distribution. There may be polar effects and pore shape effects that are important. It is recommended that some GB and/or HD isotherm data be measured on selected inorganic adsorbents and to compare these data with 2-hexanol.

2. Investigate more adsorbents by examining chromatographic column packings. The best performance is expected with linear or slightly favorable isotherms with low heat of adsorption for nerve and blister agents. Even though these materials are typically quite expensive, small amounts can lead to those characteristics that are most desirable.

3. Choose better simulants for both high volatility toxic vapors. CK loadings on silica gel are much greater than measured for R123-A at the same partial pressures and temperatures. Thus, for evaluating light gases, we need to establish the relationship between simulant and threat vapor more accurately.

4. Study the effect of relative humidity. The experiments reported here were conducted under dry conditions in the interest of testing as wide a range of adsorbents as possible. Now that the interest is focused (on silica gels), running humidified experiments is in order. One of the advantages of the test system is that it can be easily modified to perform experiments at a desired RH.

5. Model data measured in Phase I (for non-reacting only) using isotherm data and the existing mathematical model for fixed-bed adsorbers. The model, if validated based on 2-hexanol, can then be used estimate the behavior of GB and HD on the same adsorbents. It will also help to guide us toward better adsorbents.

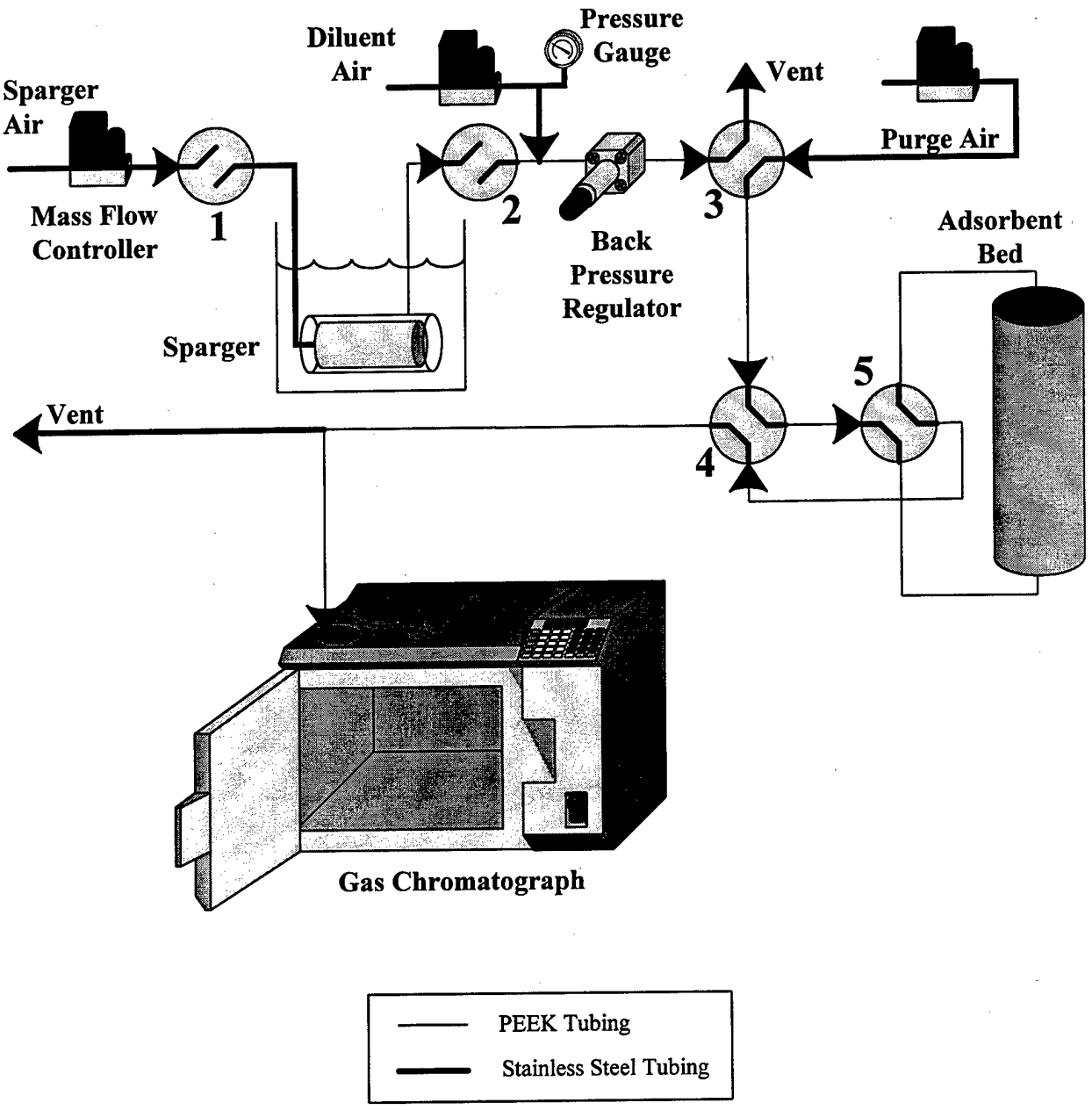

Figure 1. Schematic for Adsorption-Desorption System

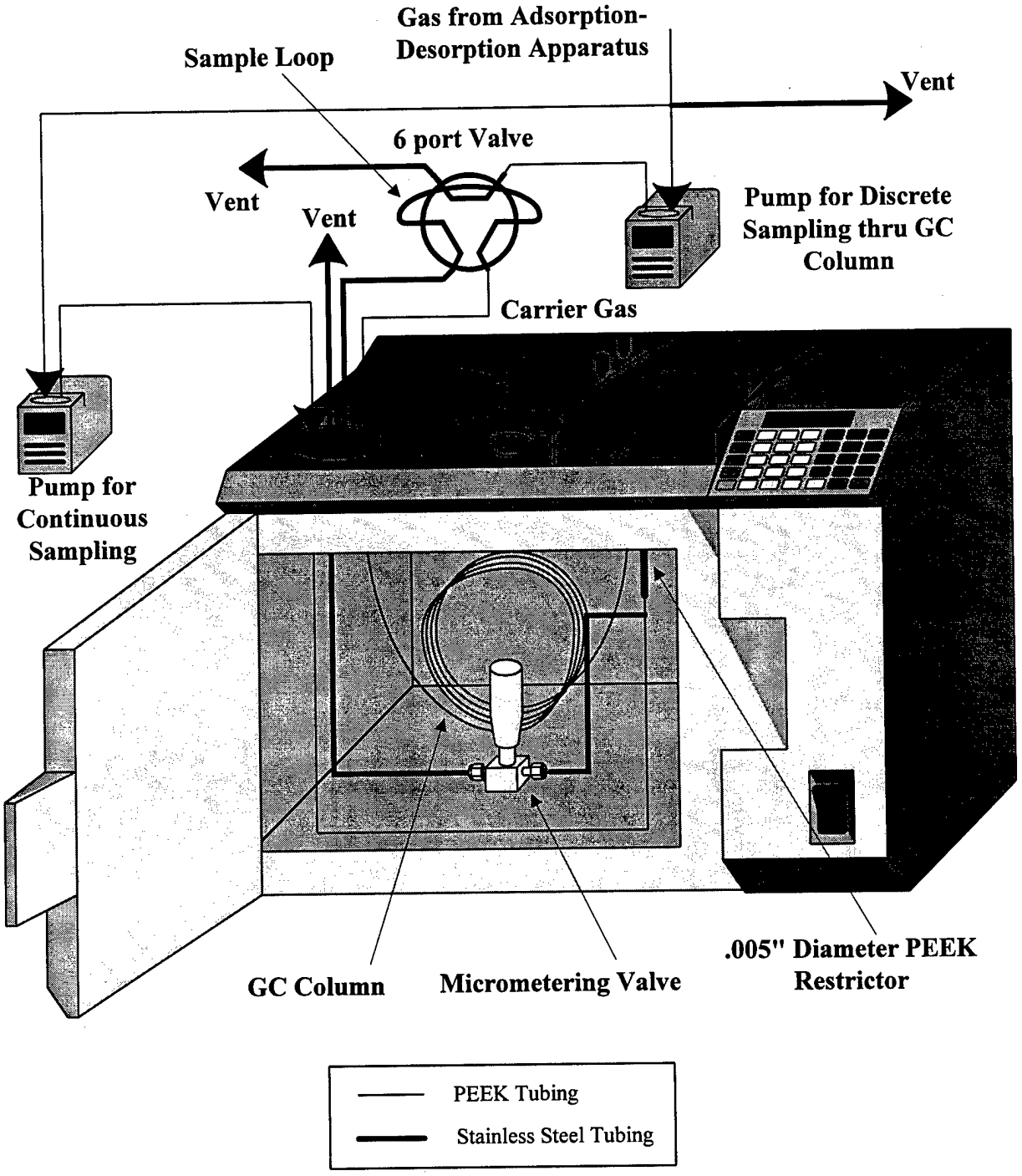

Figure 2. Analysis for Adsorption-Desorption System

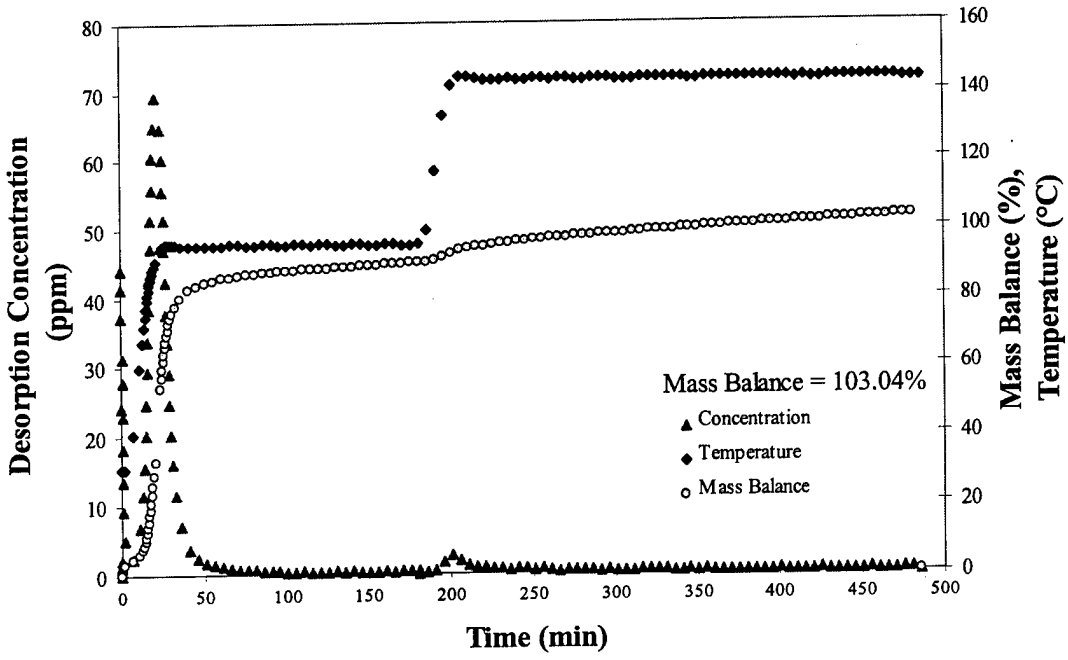

Figure 3. An Example of a Complete Desorption Experiment. Desorption of 7,000 Ct (mg-min/m^3) 2-hexanol on 12x20 Mesh Sorbead RF at 100°C and 910 ml/min.

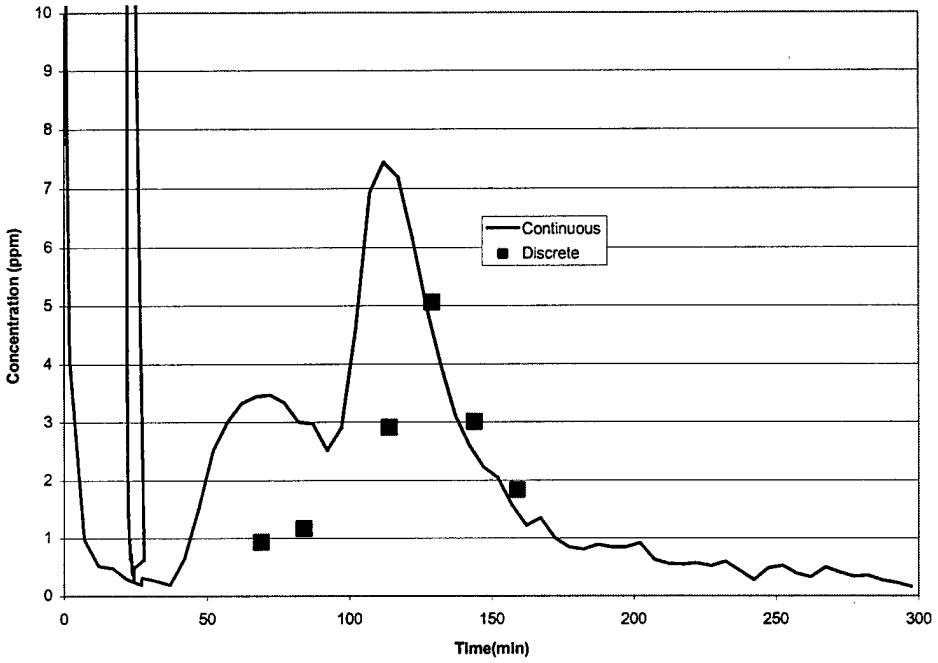

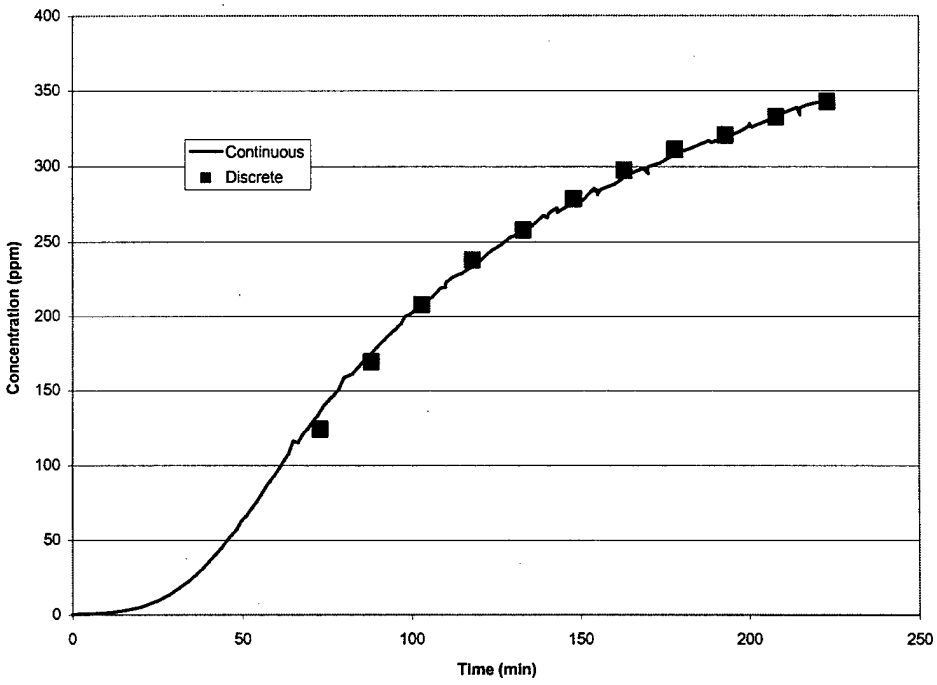

Figure 4. Experiment No. 32 Results. Desorption (Top) and Breakthrough (Bottom) Results for Alumina with a 7,000 Ct Challenge.

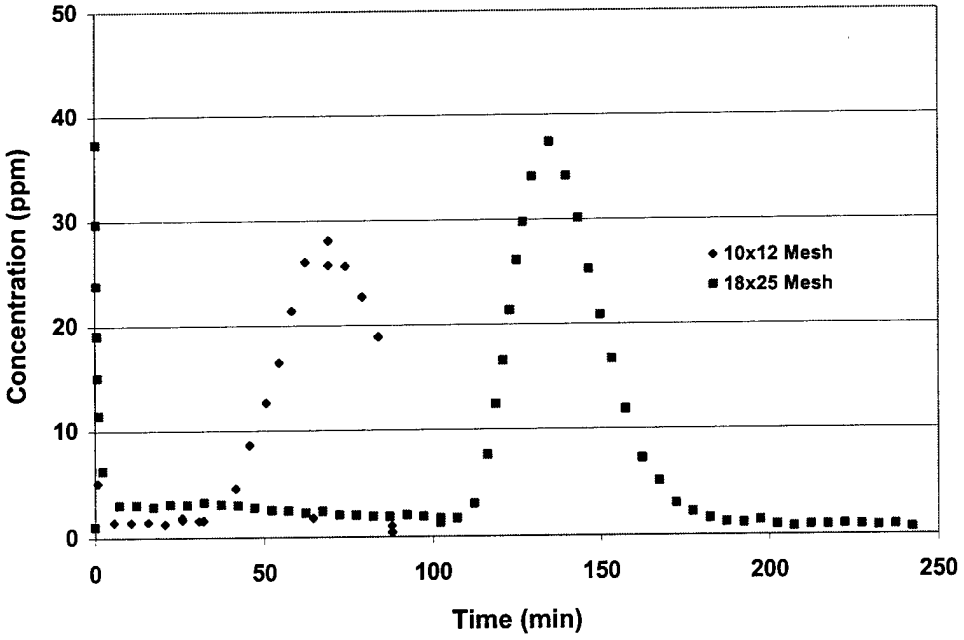

Figure 5. Comparison of Silica Gel 40 Runs (11/18/98 and 11/20/98).

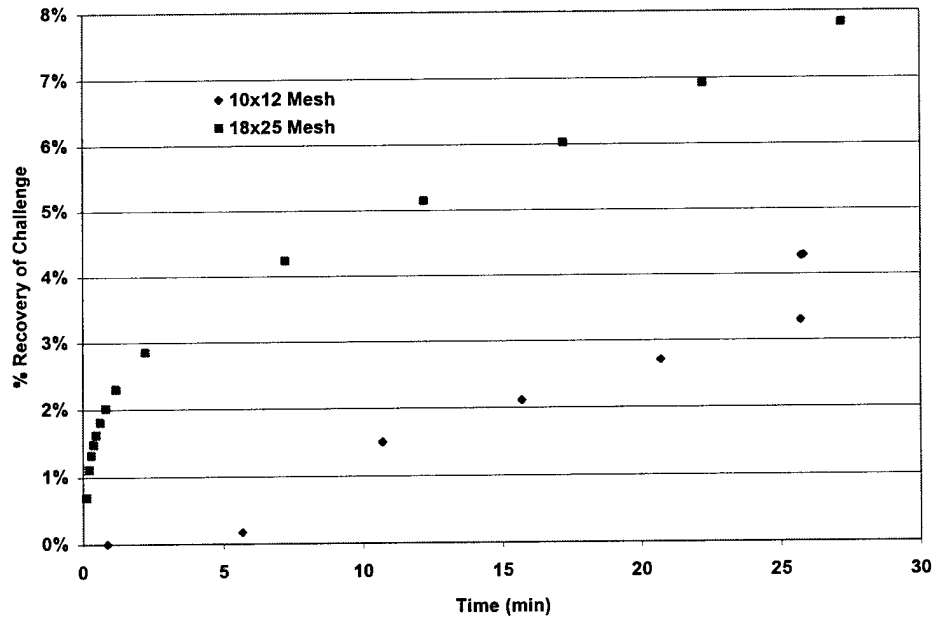

Figure 6. Progress Towards Mass Balance Closure for Silica Gel 40.

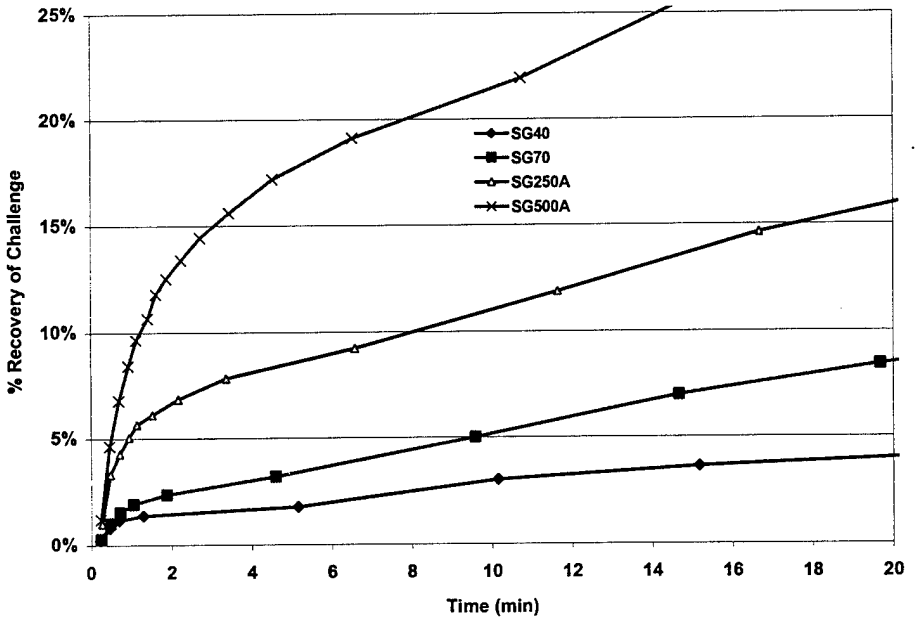

Figure 7. Comparison of Closure Rate of Mass Balance for Silica Gels.

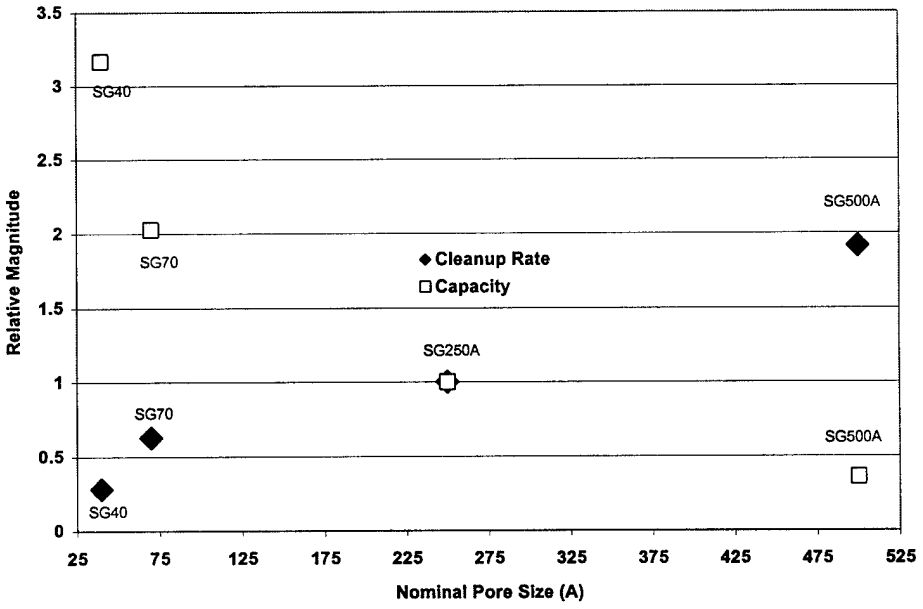

Figure 8. Comparison of Desorption Rates and Adsorption Capacities.

Blank

APPENDIX A

ADSORPTION/DESORPTION EXPERIMENTS

The following figures present data reported in Table 1. Refer to the discussion of Figure 3 for a discussion of the figures at the top of the pages. The figures at the bottom of the pages (when present) show breakthrough and the calculated accumulation of adsorbate in the bed.

There are more adsorption-desorption experiments than breakthrough experiments because breakthrough experiments were not rerun when a different desorption temperature was used for an adsorption-desorption experiment.

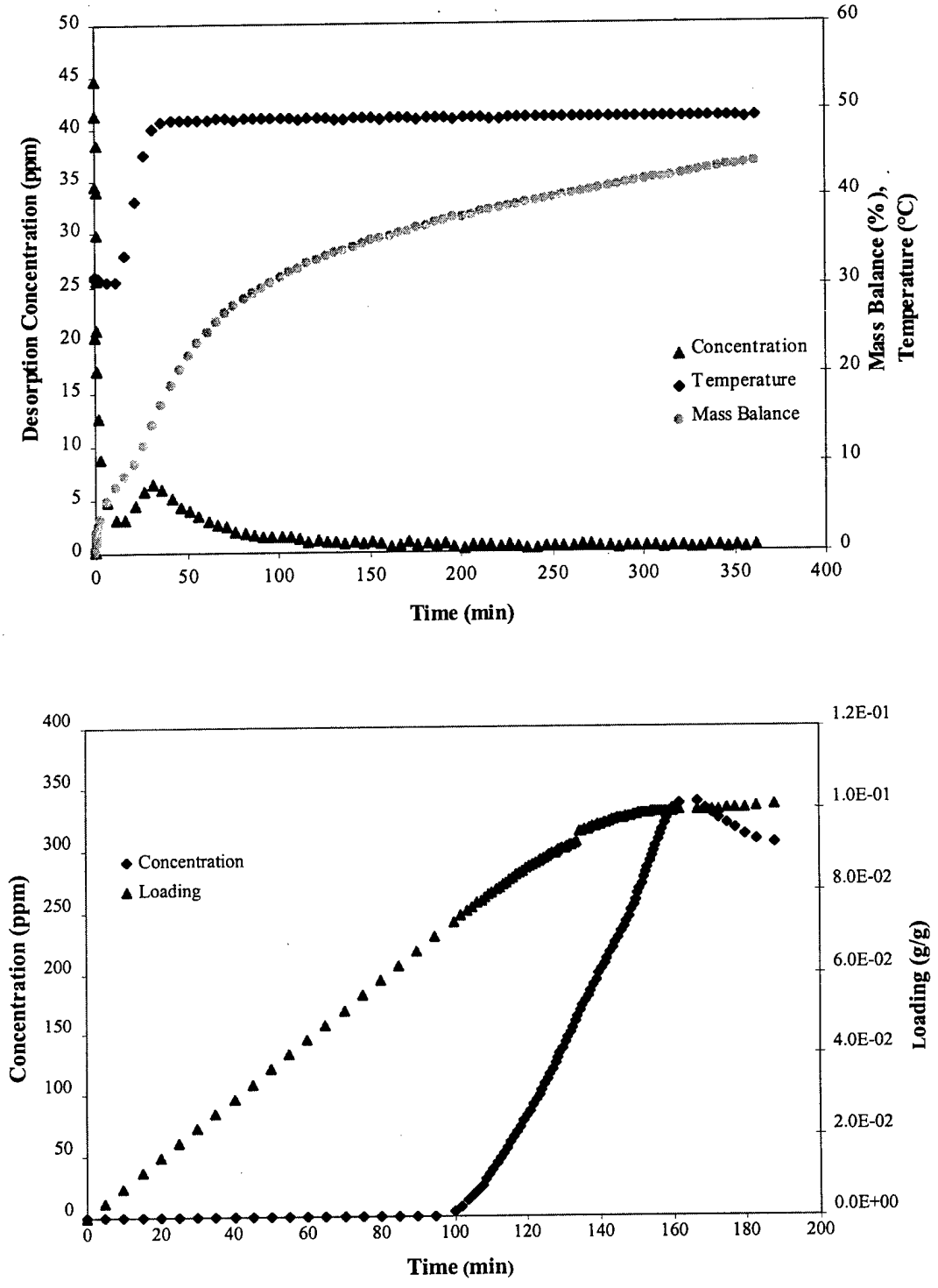

Figure A1. Experiment No. 1 Results. Desorption (Top) and Breakthrough (Bottom) Results for Silica Gel 250Å with a 7,000 Ct Challenge.

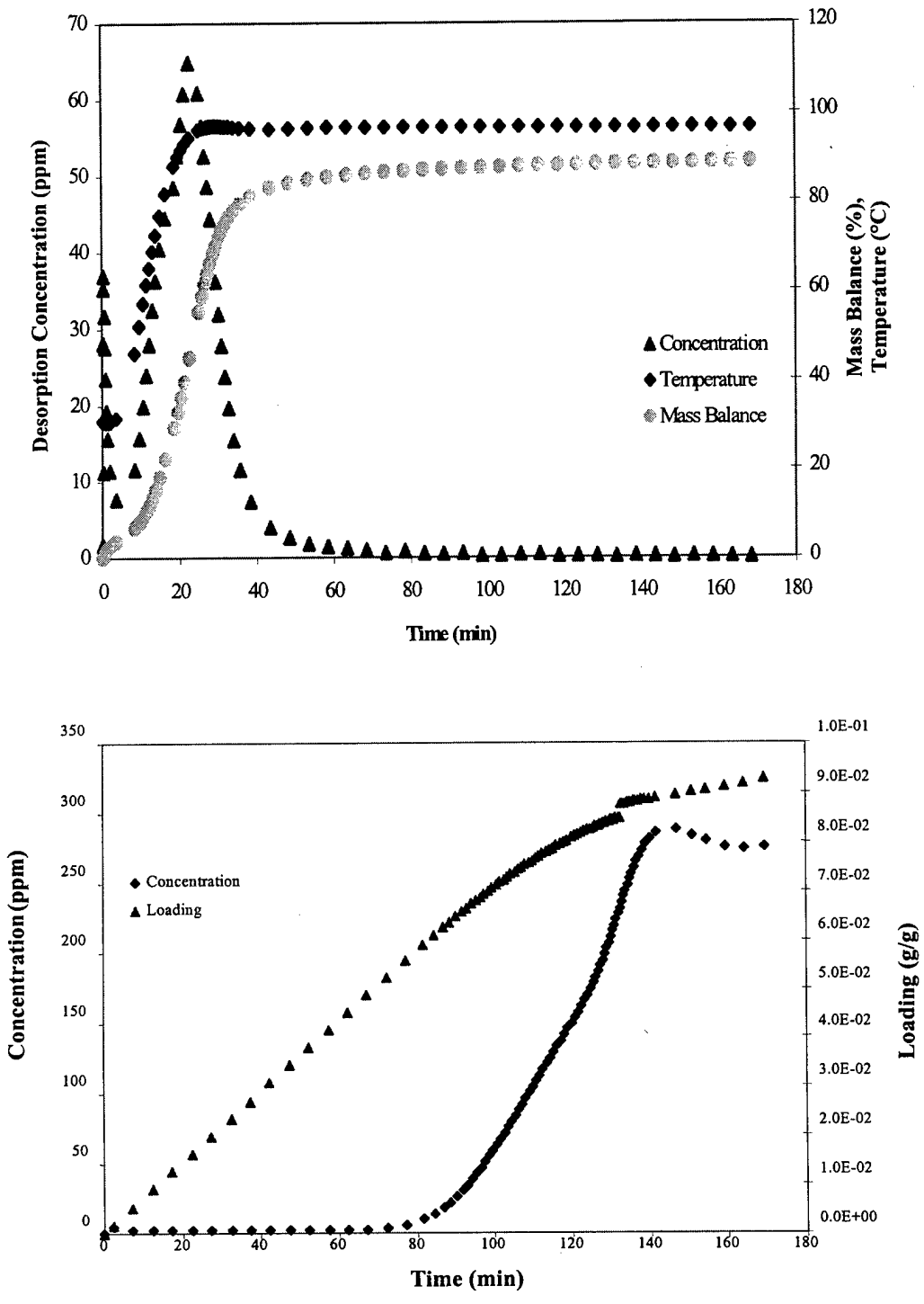

Figure A.2. Experiment No. 2 Results. Desorption (Top) and Breakthrough (Bottom) Results for Silica Gel 250Å with a 7,000 Ct Challenge.

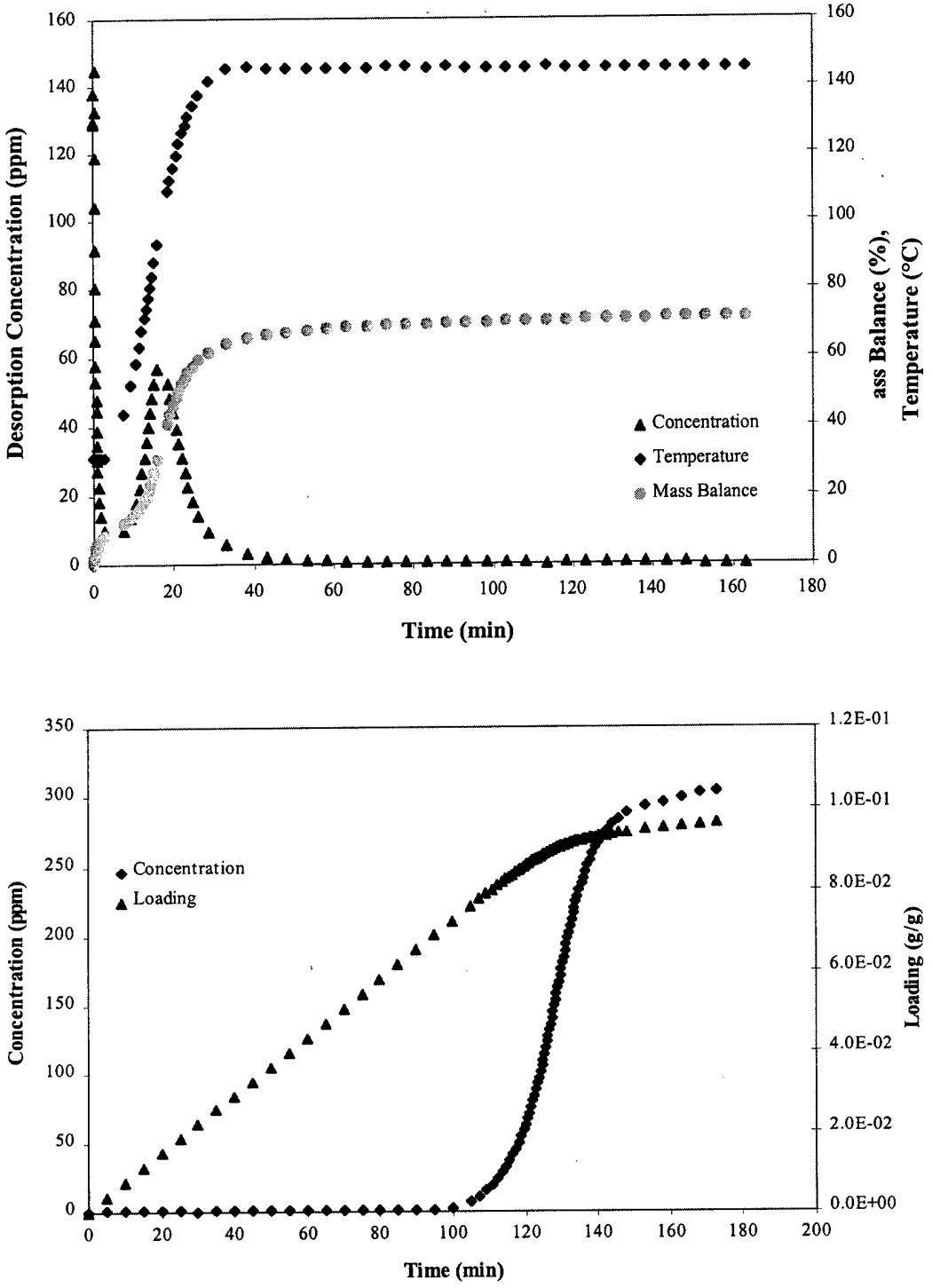

Figure A.3. Experiment No. 3 Results. Desorption (Top) and Breakthrough (Bottom) Results for Silica Gel 250Å with a 7,000 Ct Challenge.

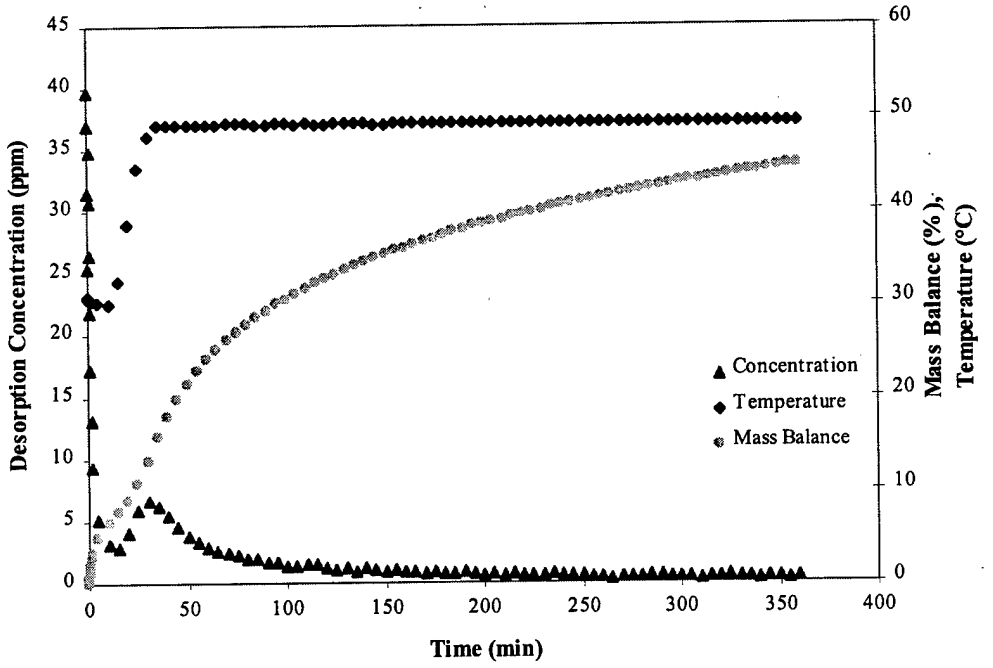

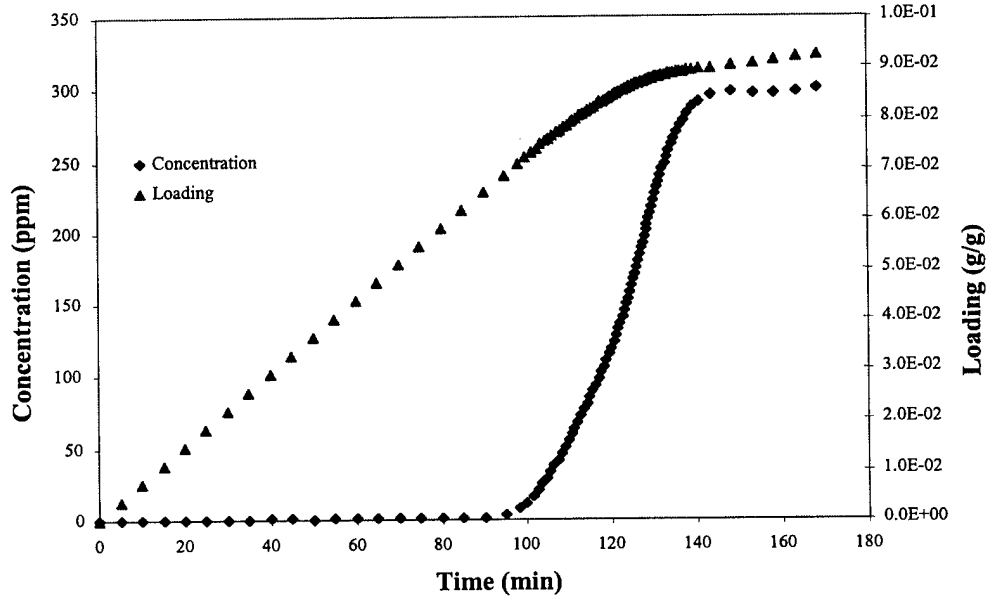

Figure A.4. Experiment No. 4 Results. Desorption (Top) and Breakthrough (Bottom) Results for Silica Gel 250Å with a 7,000 Ct Challenge.

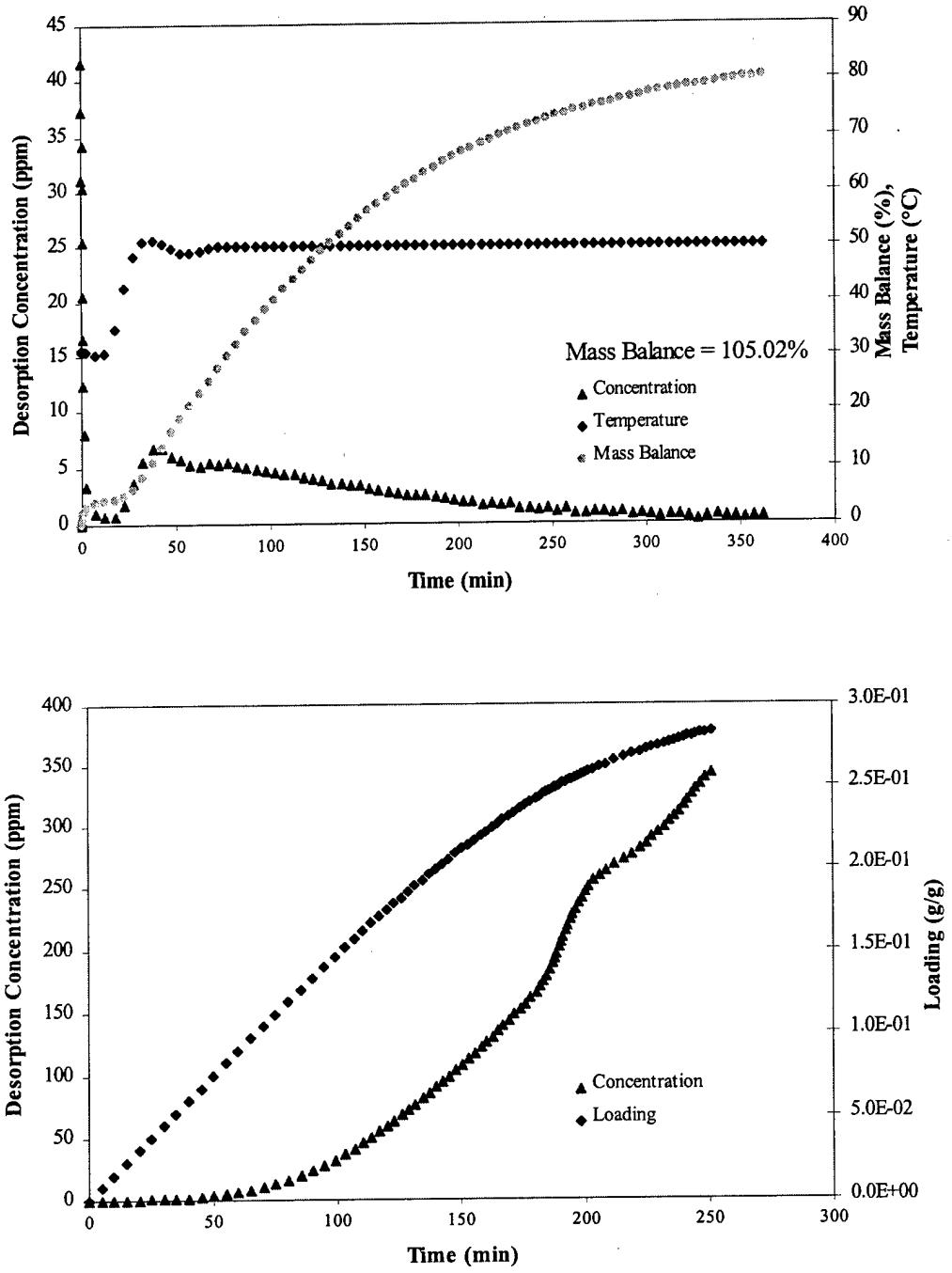

Figure A.5. Experiment No. 5 Results. Desorption (Top) and Breakthrough (Bottom) Results for Sorbead RF with a 7,000 Ct Challenge.

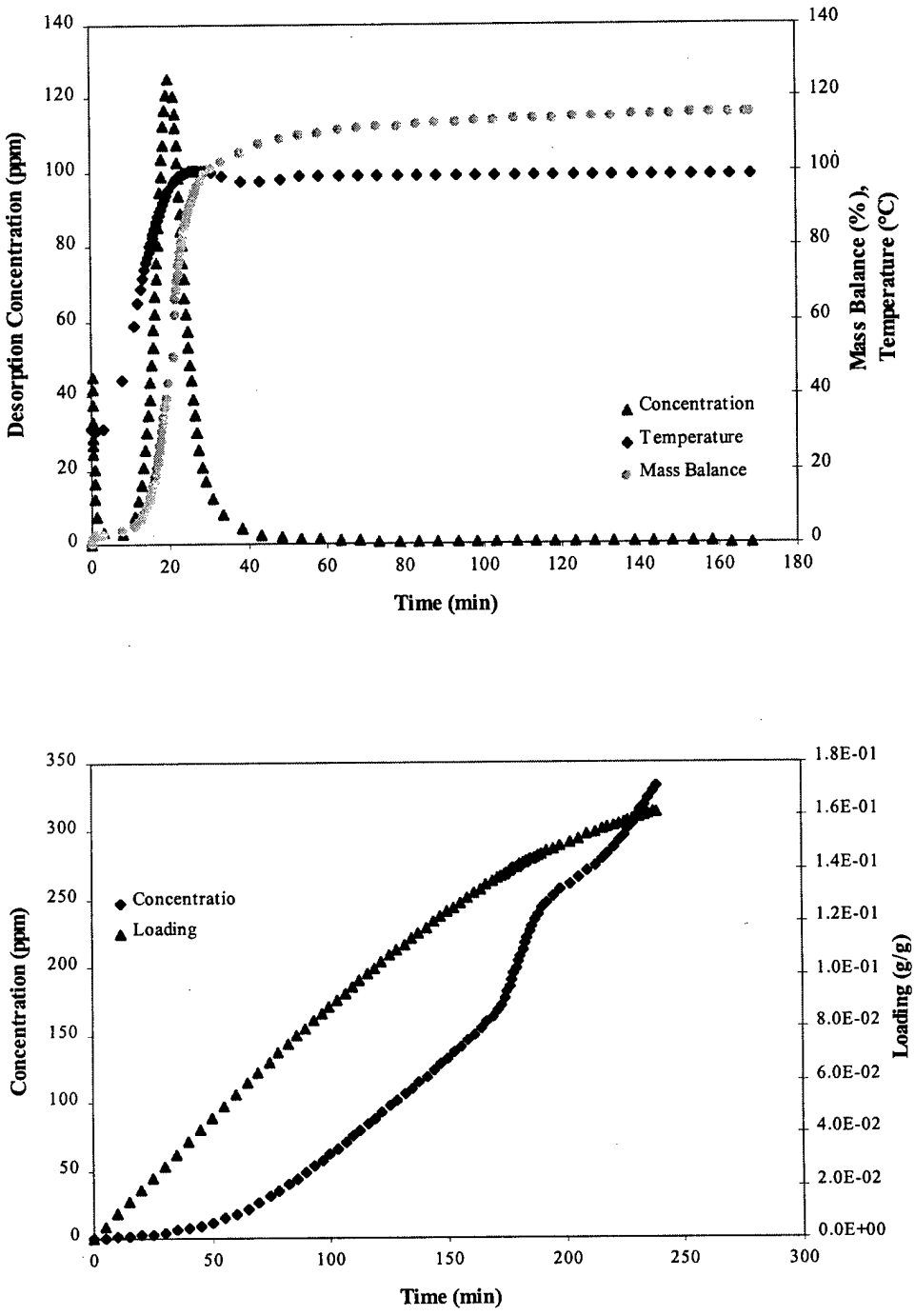

Figure A.6. Experiment No. 6 Results. Desorption (Top) and Breakthrough (Bottom) Results for Sorbead RF with a 7,000 Ct Challenge.

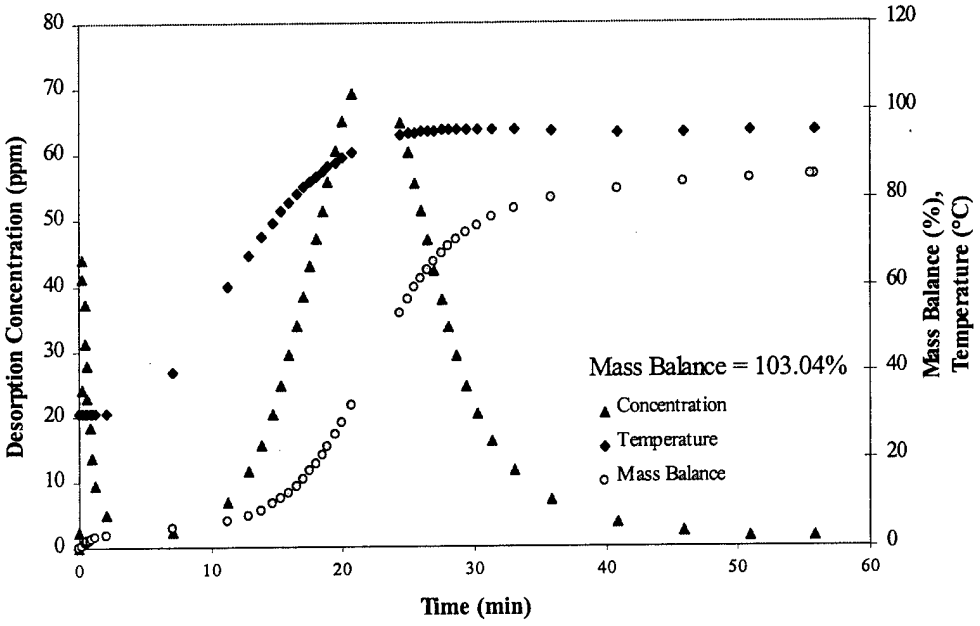

Figure A.7. Experiment No. 7 Results. Desorption Results for Sorbead RF with a 7,000 Ct Challenge.

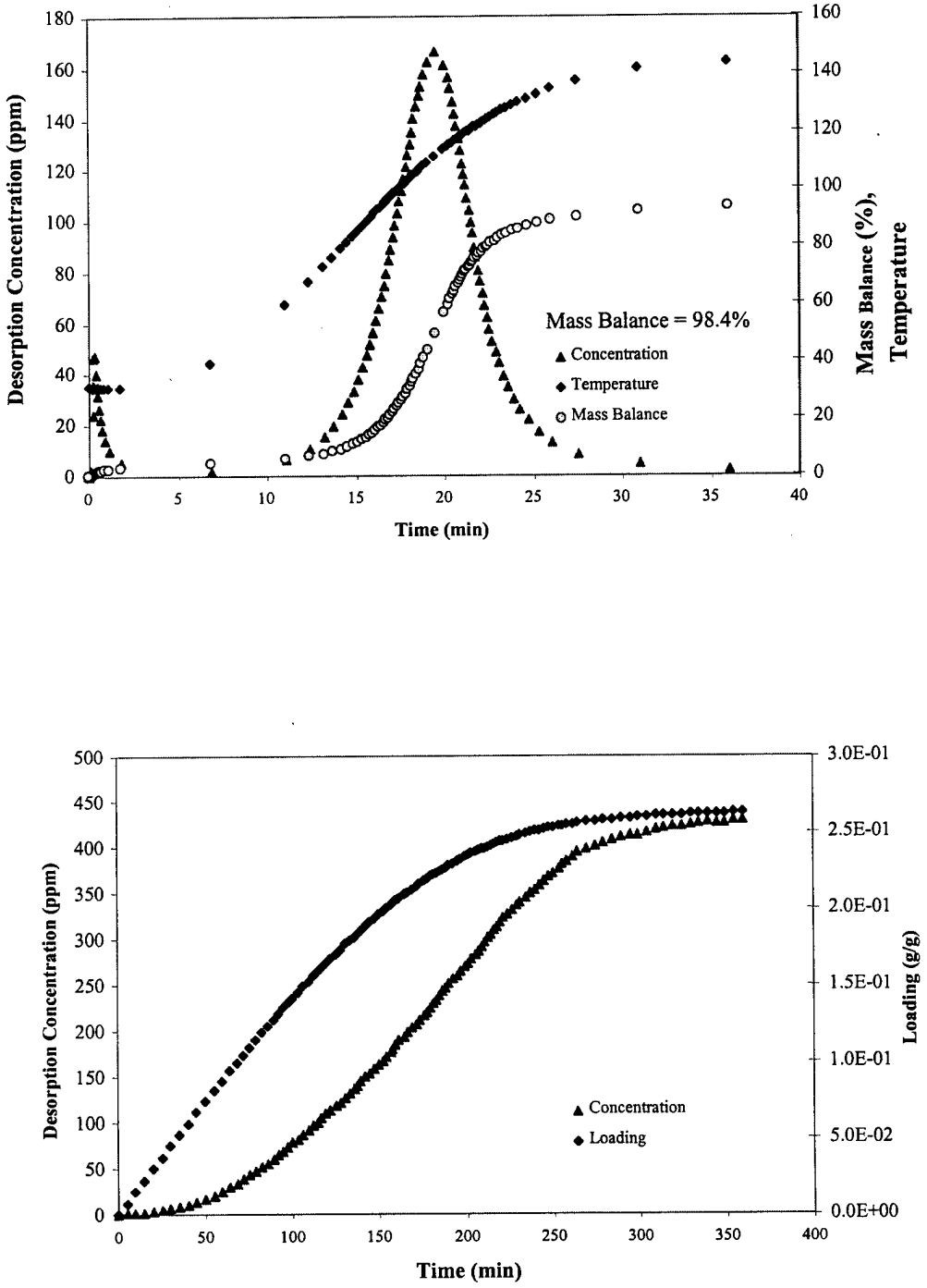

Figure A.8. Experiment No. 8 Results. Desorption (Top) and Breakthrough (Bottom) Results for Sorbead RF with a 7,000 Ct Challenge.

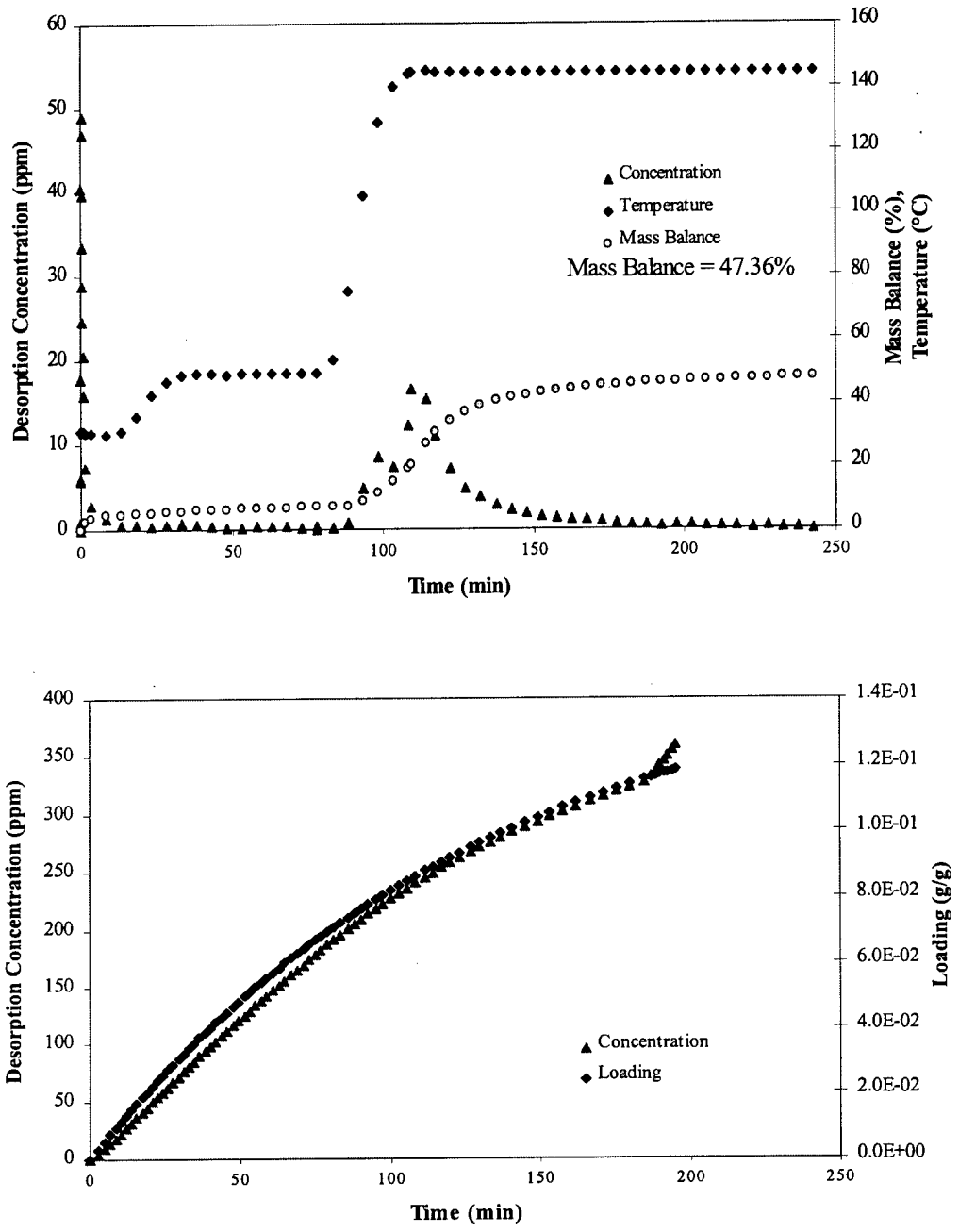

Figure A.9. Experiment No. 9 Results. Desorption (Top) and Breakthrough (Bottom) Results for Alumina with a 7,000 Ct Challenge.

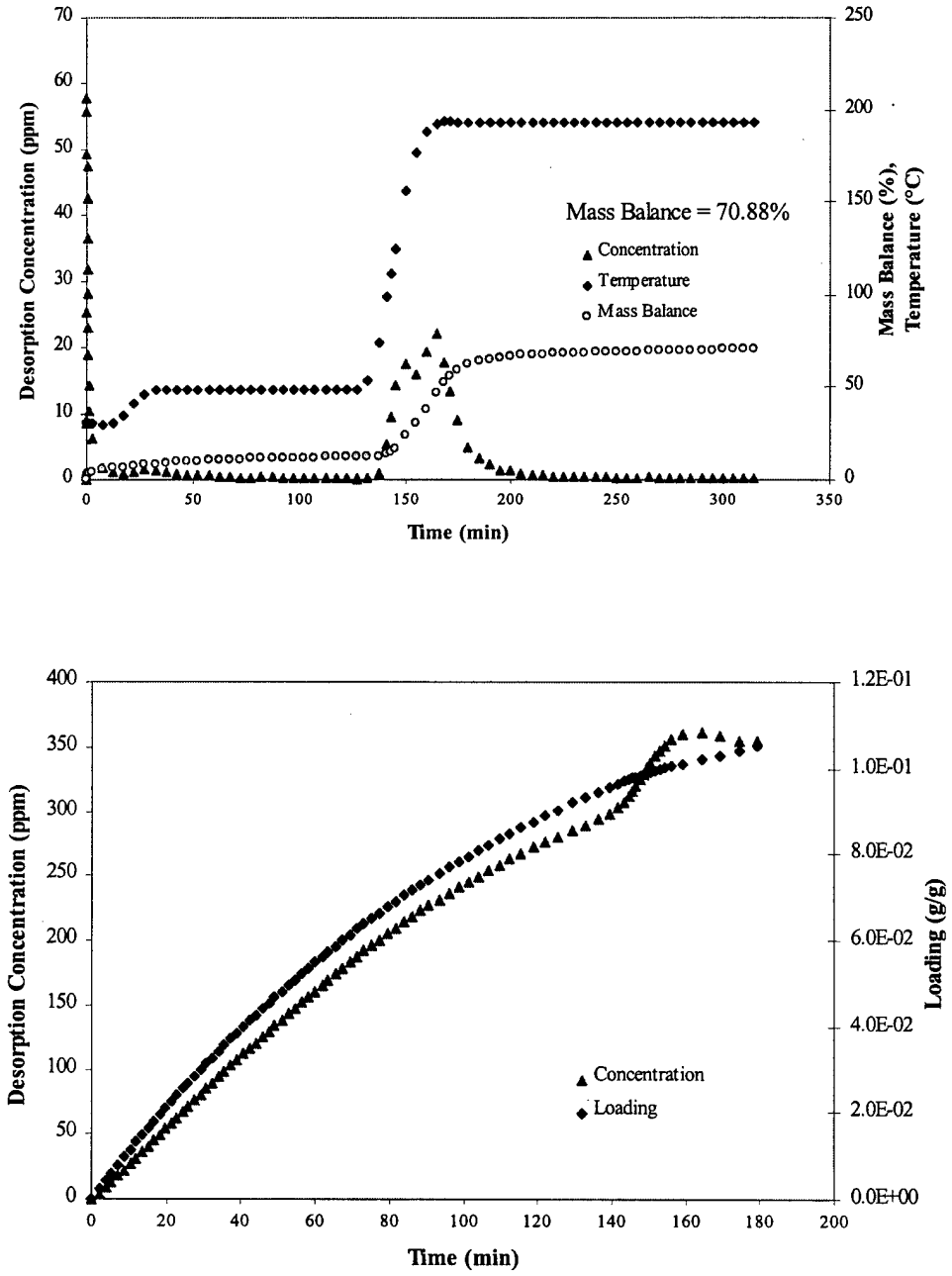

Figure A.10. Experiment No. 10 Results. Desorption (Top) and Breakthrough (Bottom) Results for Alumina with a 7,000 Ct Challenge.

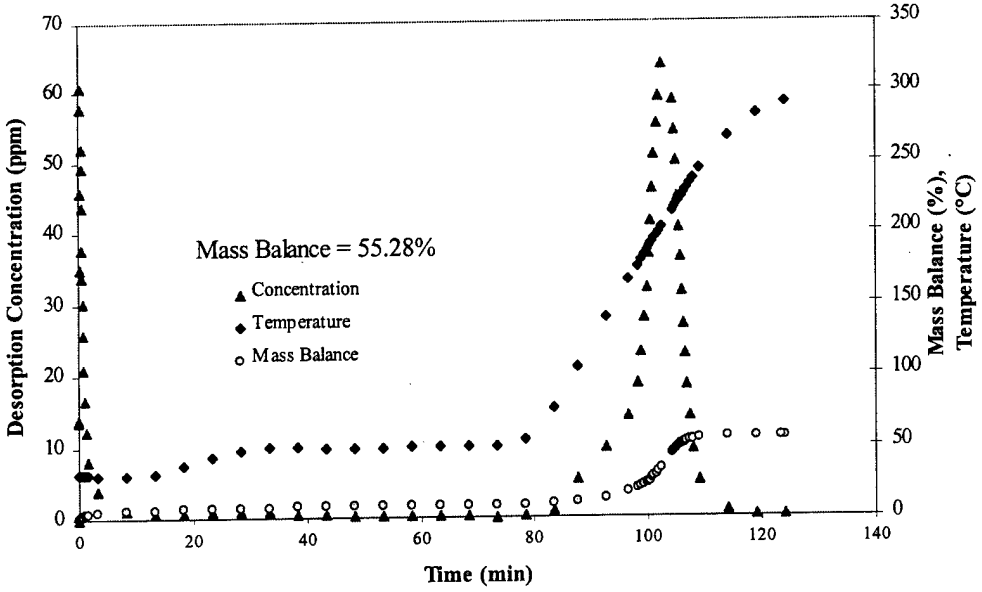

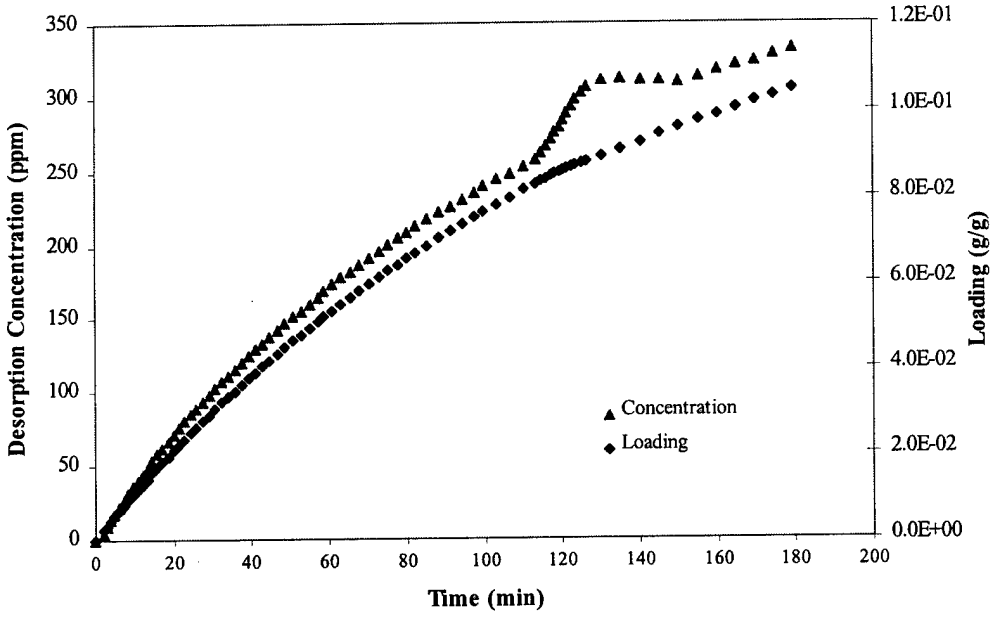

Figure A.11. Experiment No. 11 Results. Desorption (Top) and Breakthrough (Bottom) Results for Alumina with a 7,000 Ct Challenge.

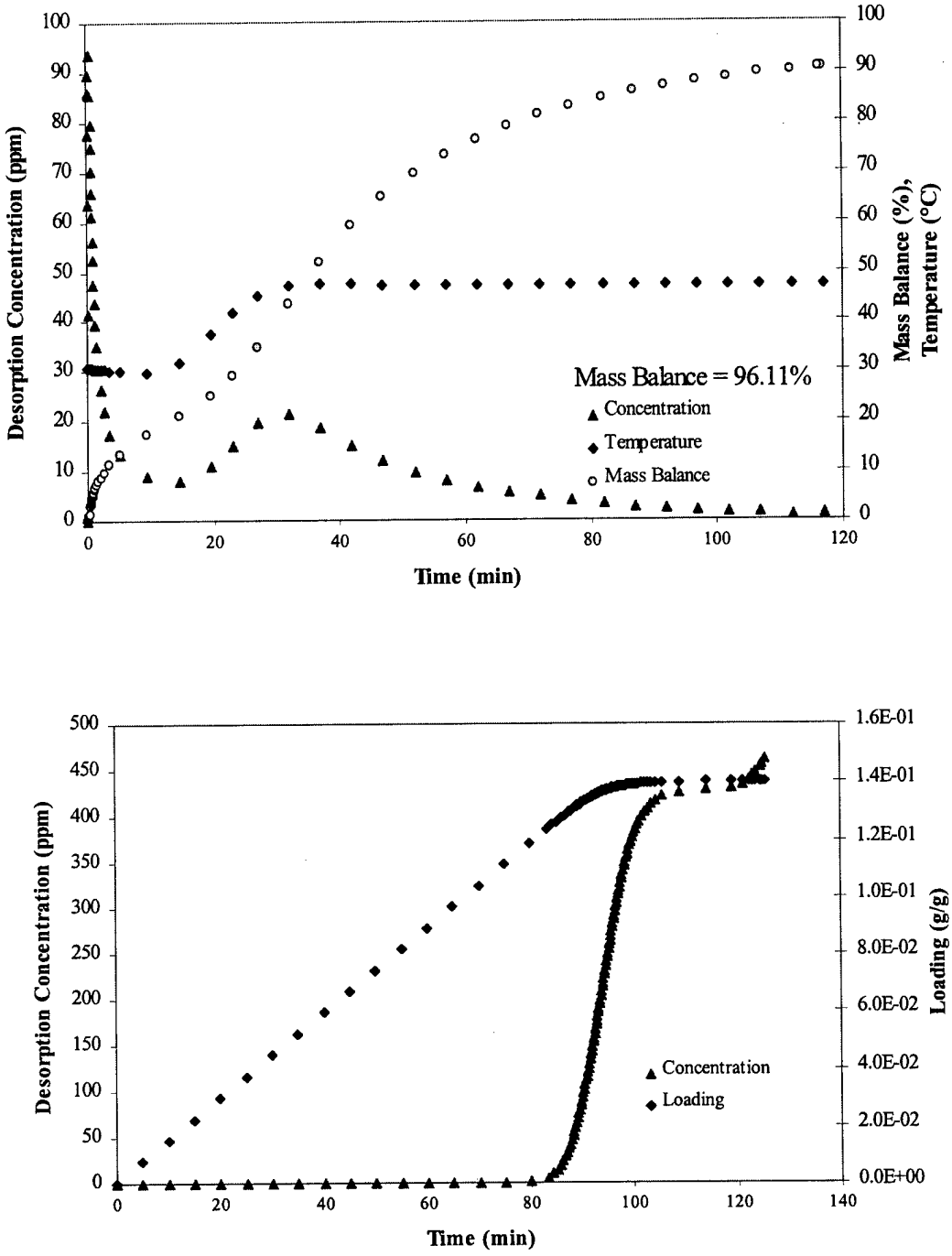

Figure A.12. Experiment No. 12 Results. Desorption (Top) and Breakthrough (Bottom) Results for Silica Gel 250Å with a 7,000 Ct Challenge.

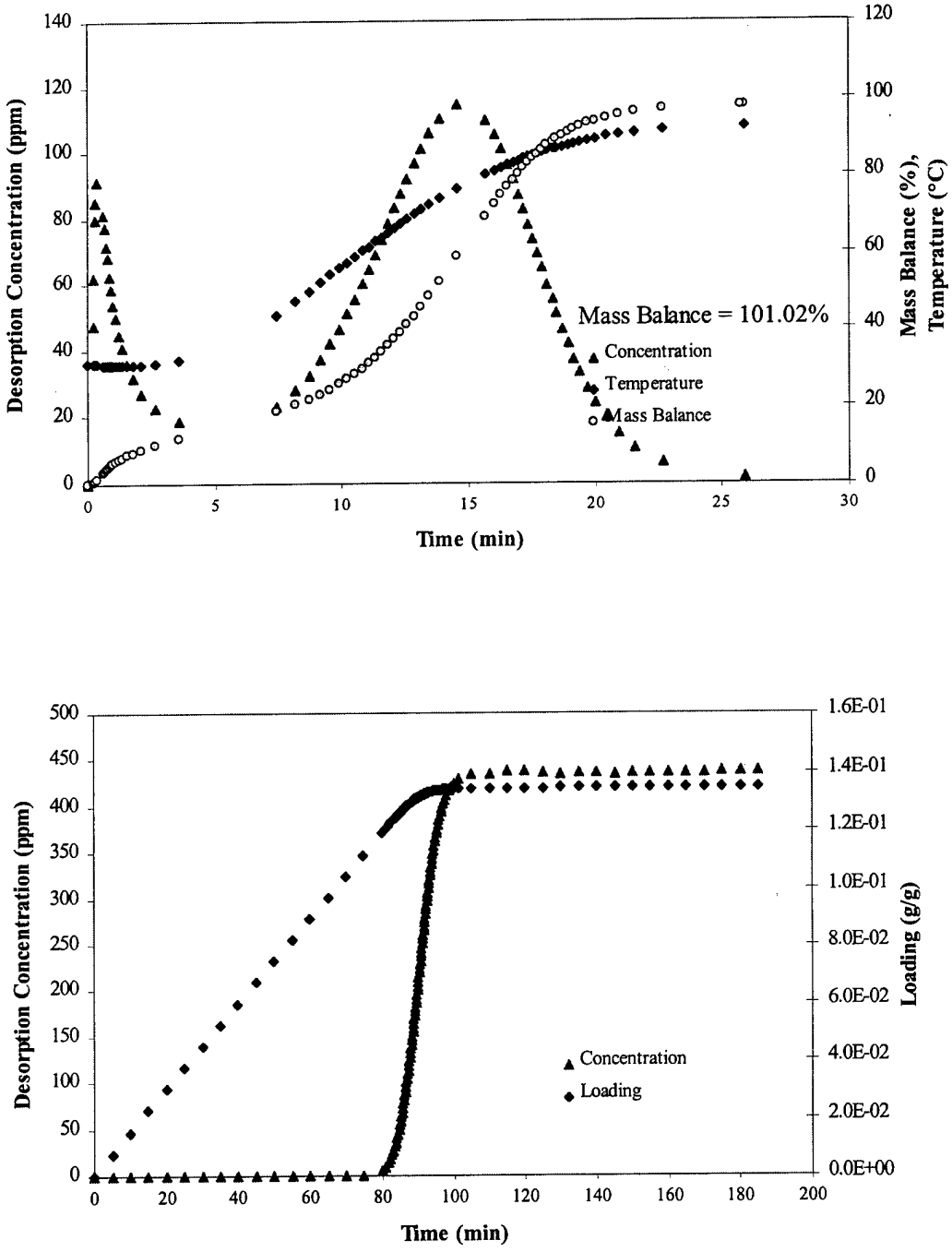

Figure A.13. Experiment No. 13 Results. Desorption (Top) and Breakthrough (Bottom) Results for Silica Gel 250Å with a 7,000 Ct Challenge.

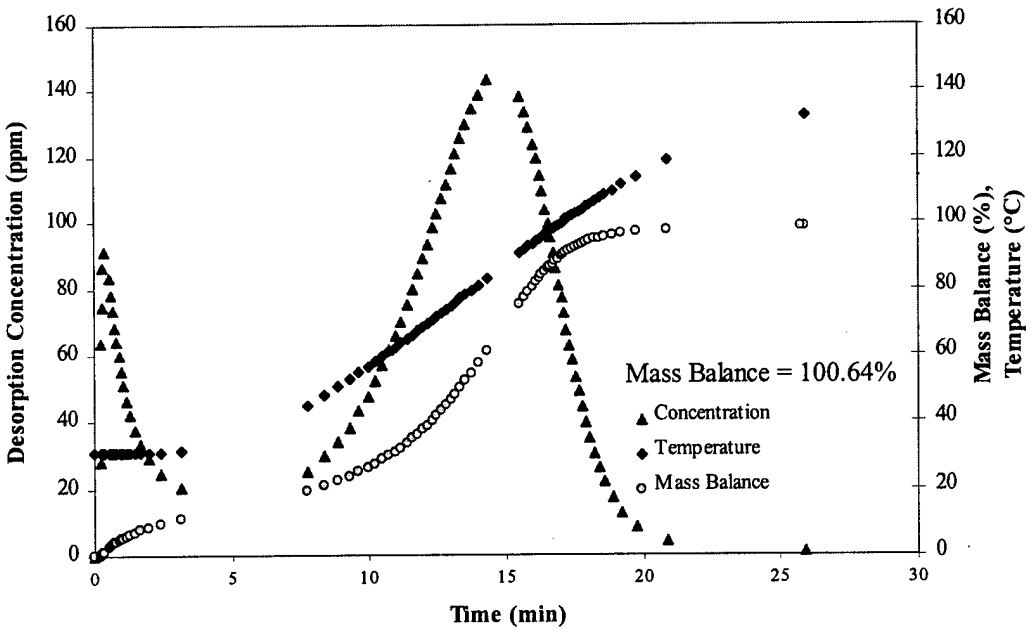

Figure A.14. Experiment No. 14 Results. Desorption Results for Silica Gel 250Å with a 7,000 Ct Challenge.

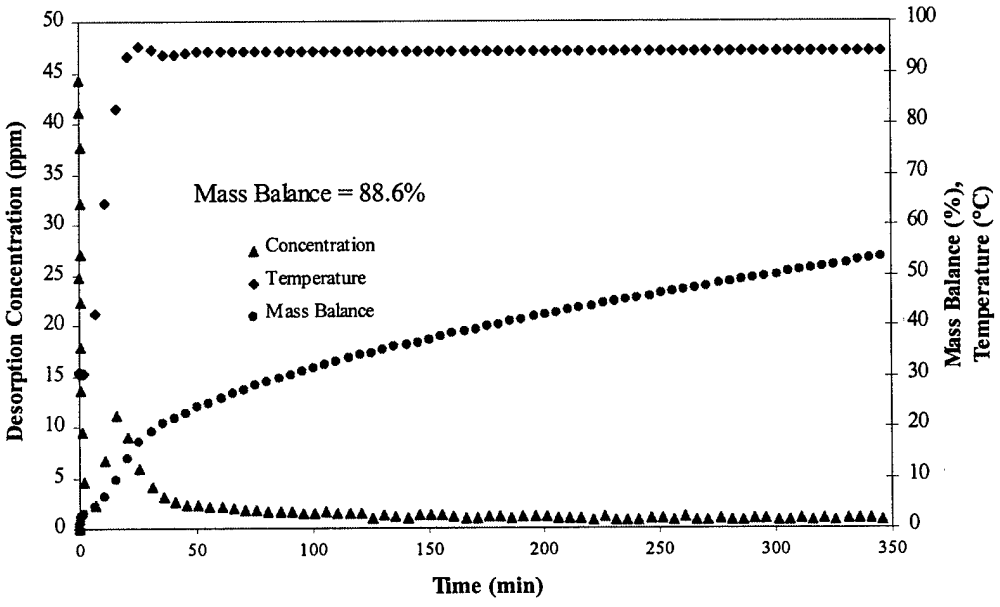

Figure A.15. Experiment No. 15 Results. Desorption Results for Alumina with a 7,000 Ct Challenge.

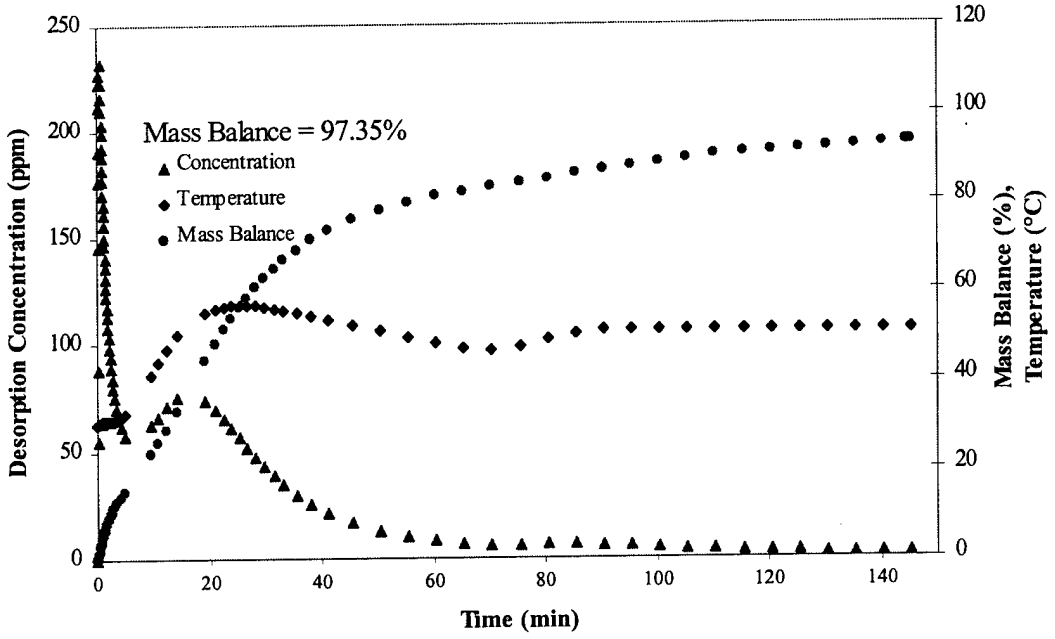

Figure A.16. Experiment No. 16 Results. Desorption Results for Silica Gel 250Å with a 20,000 Ct Challenge.

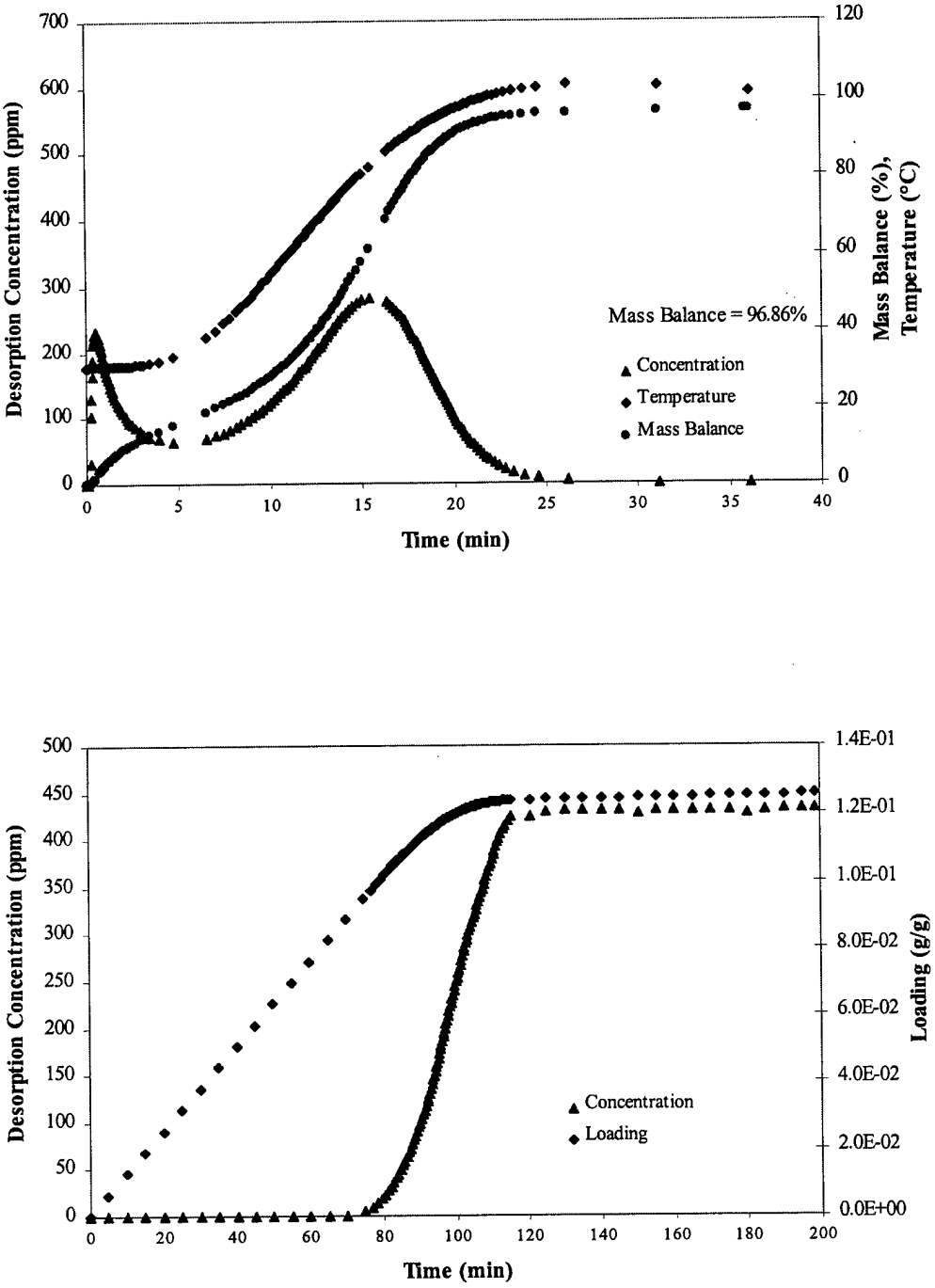

Figure A.17. Experiment No. 17 Results. Desorption (Top) and Breakthrough (Bottom) Results for Silica Gel 250Å with a 20,000 Ct Challenge.

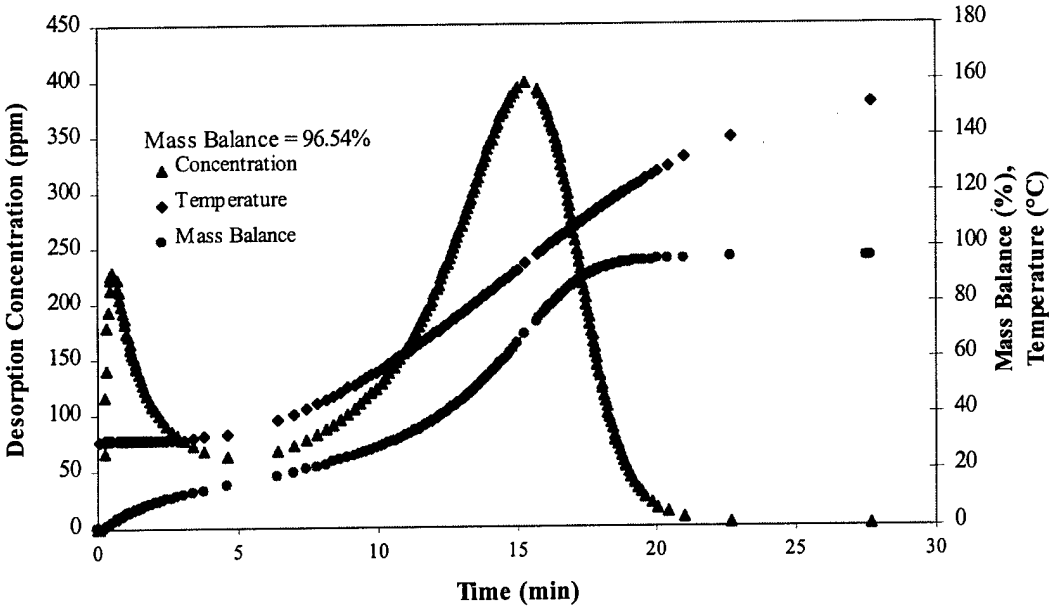

Figure A.18. Experiment No. 18 Results. Desorption Results for Silica Gel 250Å with a 20,000 Ct Challenge.

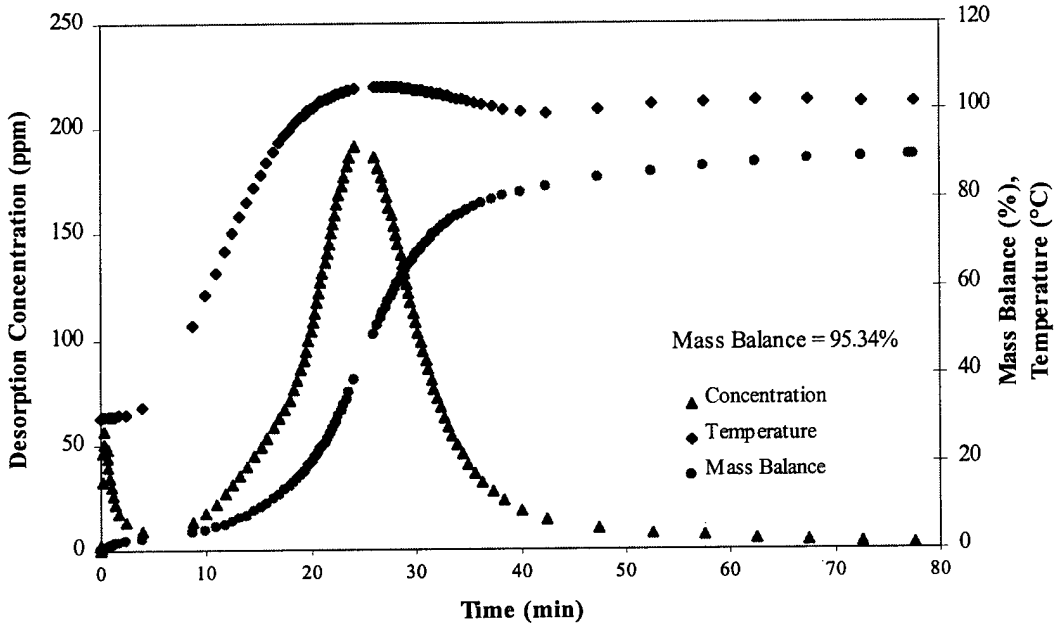

Figure A.19. Experiment No. 19 Results. Desorption Results for Sorbead RF with a 20,000 Ct Challenge.

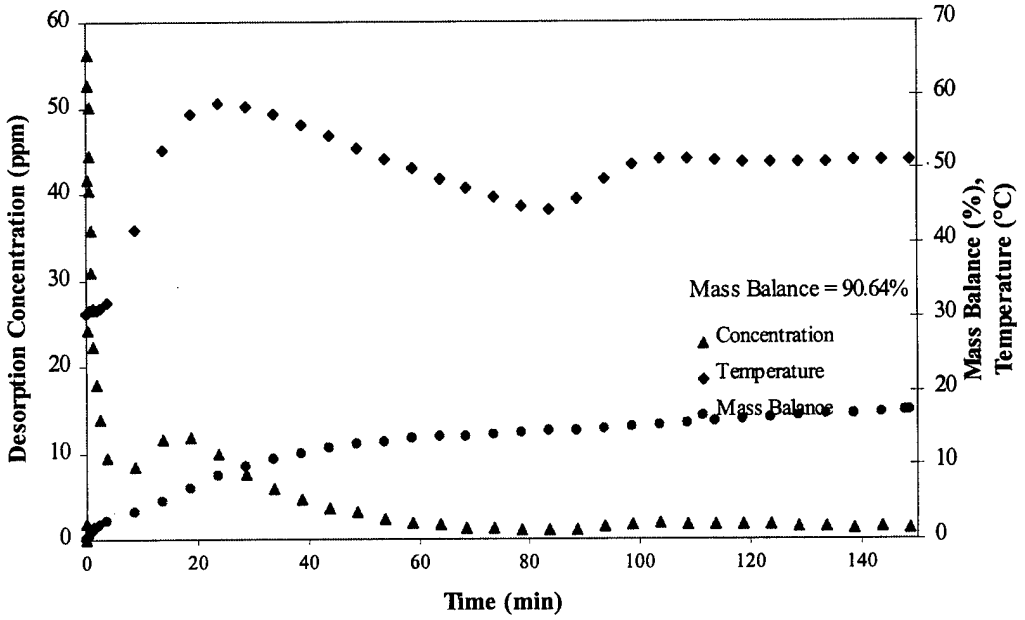

Figure A.20. Experiment No. 20 Results. Desorption Results for Sorbead RF with a 20,000 Ct Challenge.

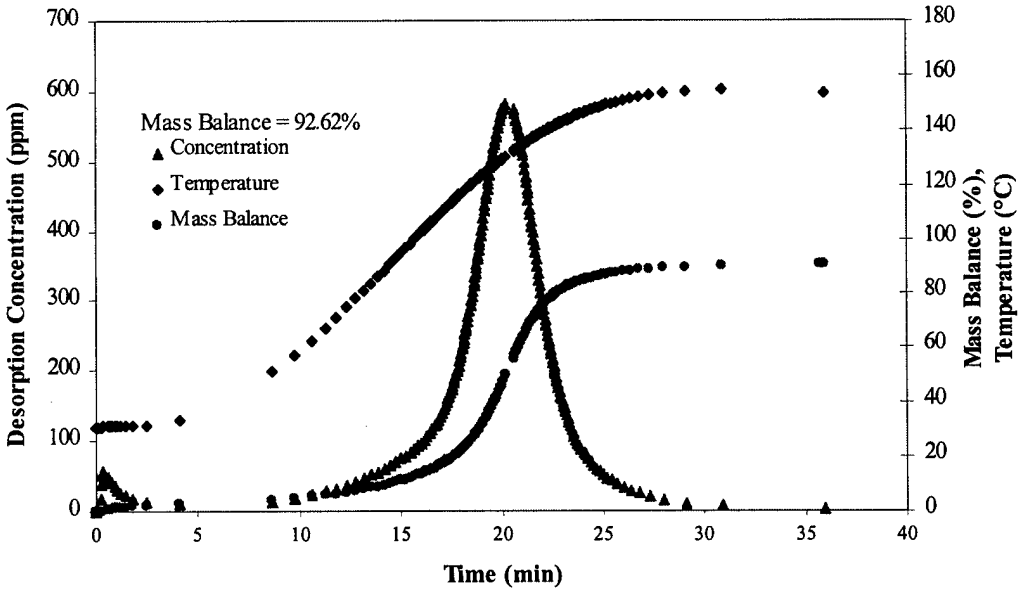

Figure A.21. Experiment No. 21 Results. Desorption Results for Sorbead RF with a 20,000 Ct Challenge.

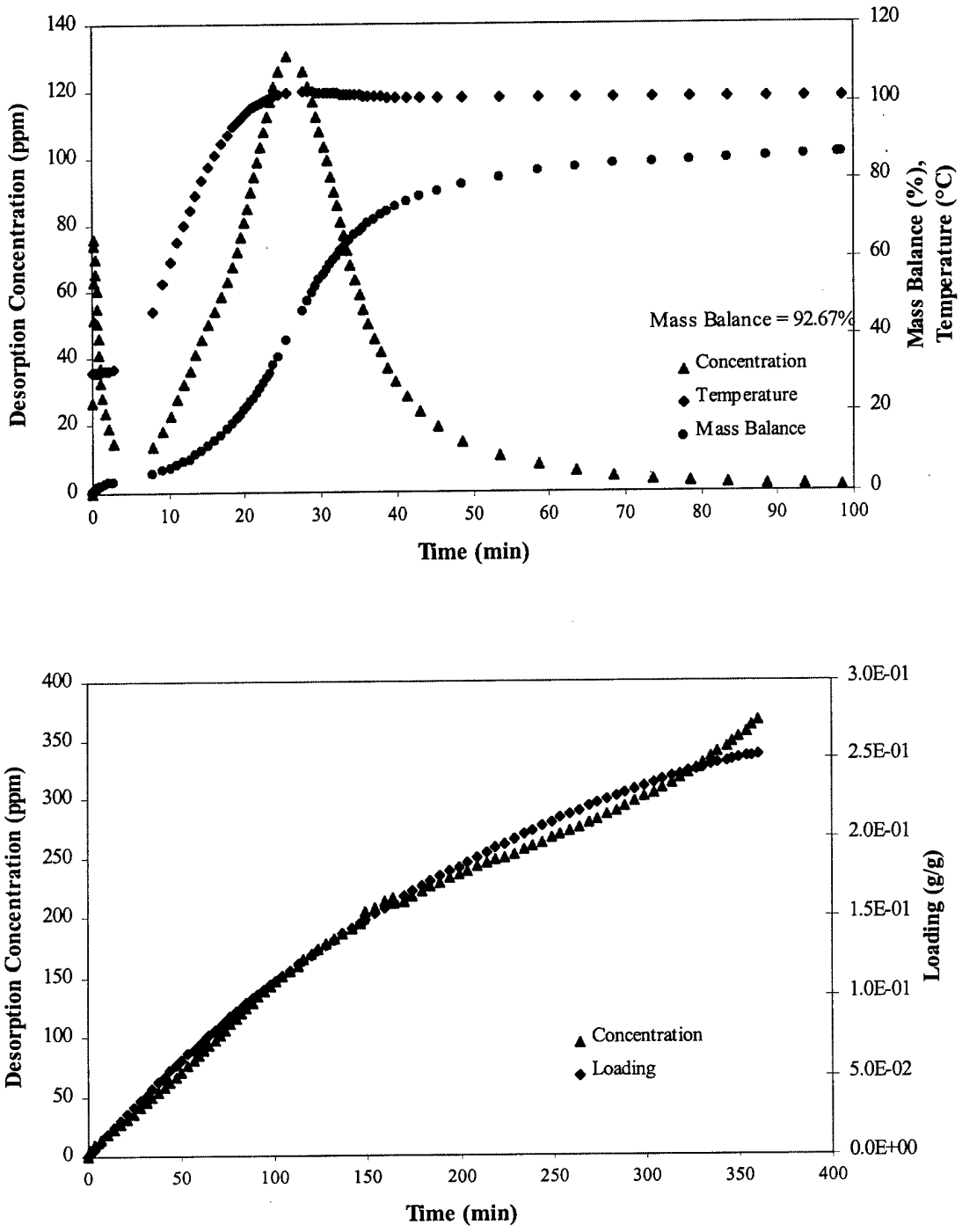

Figure A.22. Experiment No. 22 Results. Desorption (Top) and Breakthrough (Bottom) Results for Calcined Sorbead RF with a 20,000 Ct Challenge.

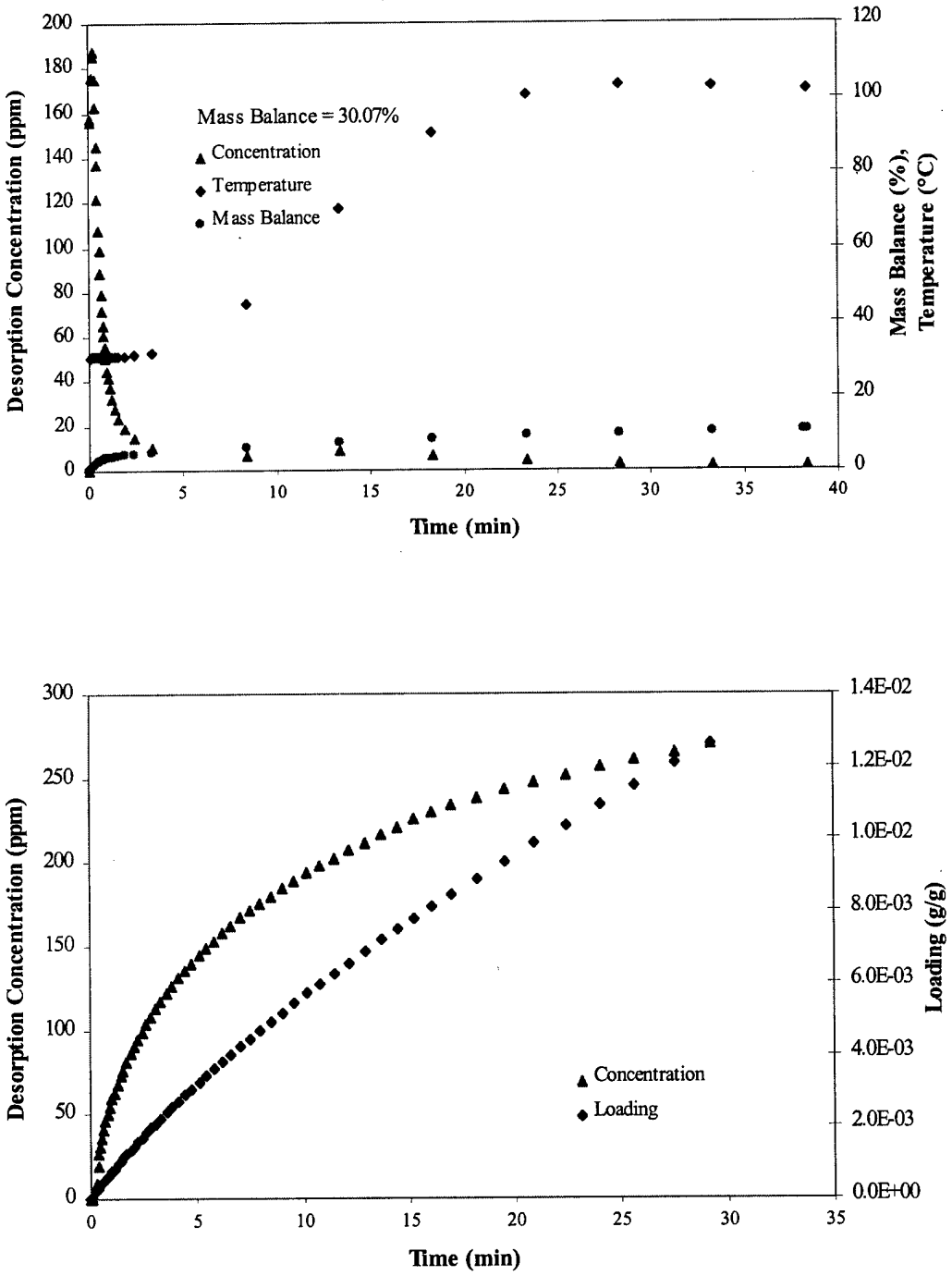

Figure A.23. Experiment No. 23 Results. Desorption (Top) and Breakthrough (Bottom) Results for Zirconia (XZ 16122) with a 20,000 Ct Challenge.

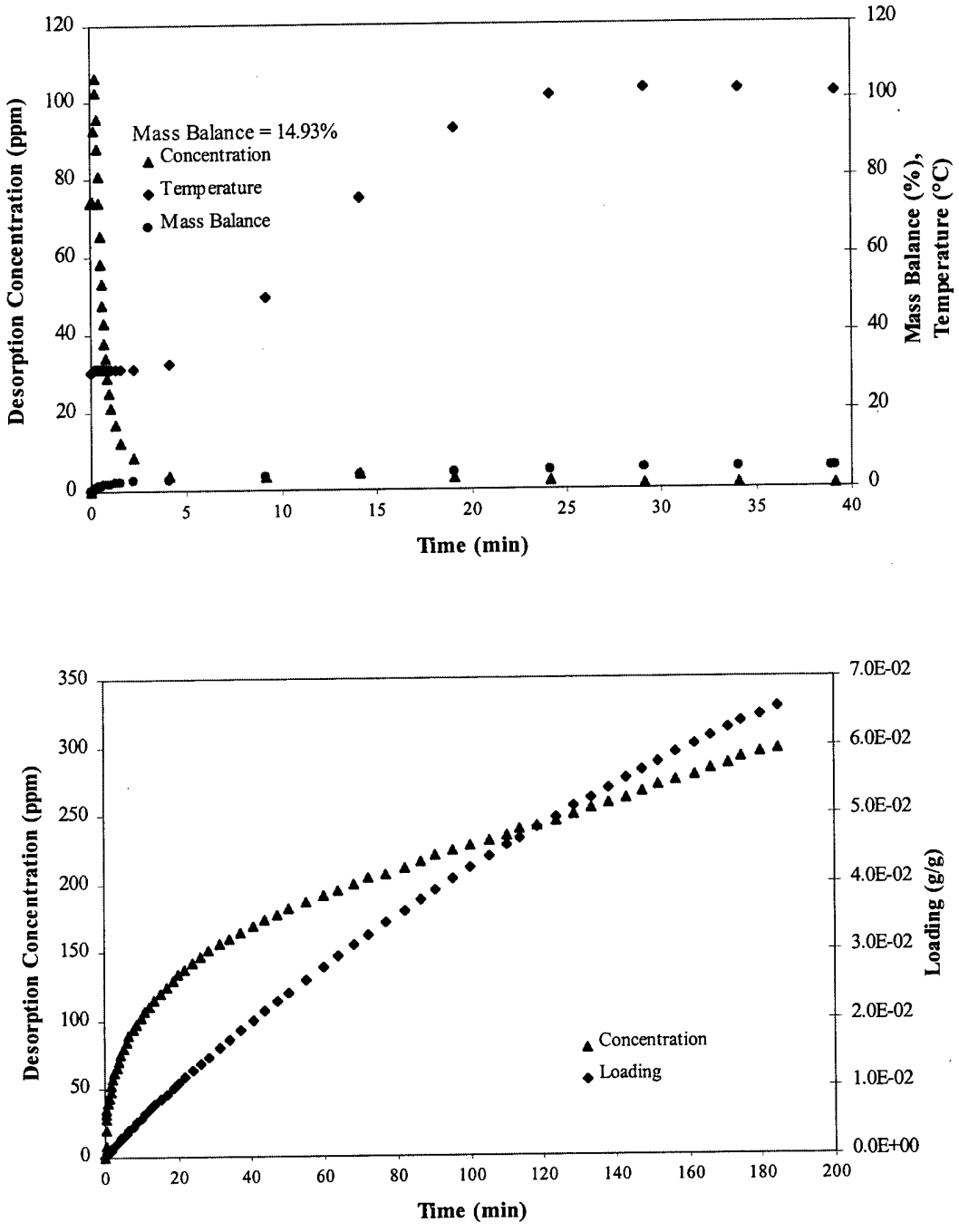

Figure A.24. Experiment No. 24 Results. Desorption (Top) and Breakthrough (Bottom) Results for Zirconia (XZ 16154) with a 20,000 Ct Challenge.

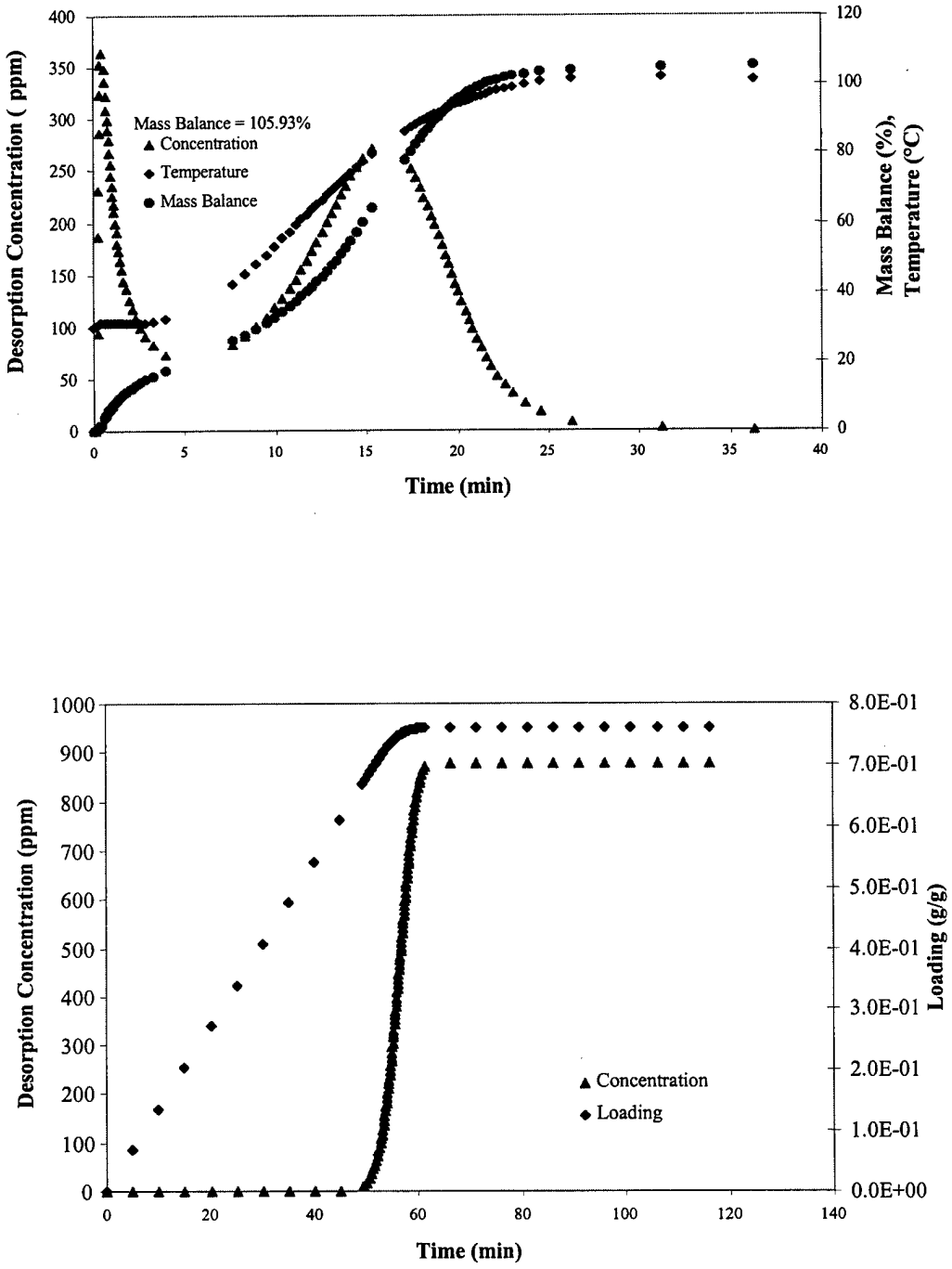

Figure A.25. Experiment No. 25 Results. Desorption (Top) and Breakthrough (Bottom) Results for Silica Gel 250Å with a 20,000 Ct Challenge.

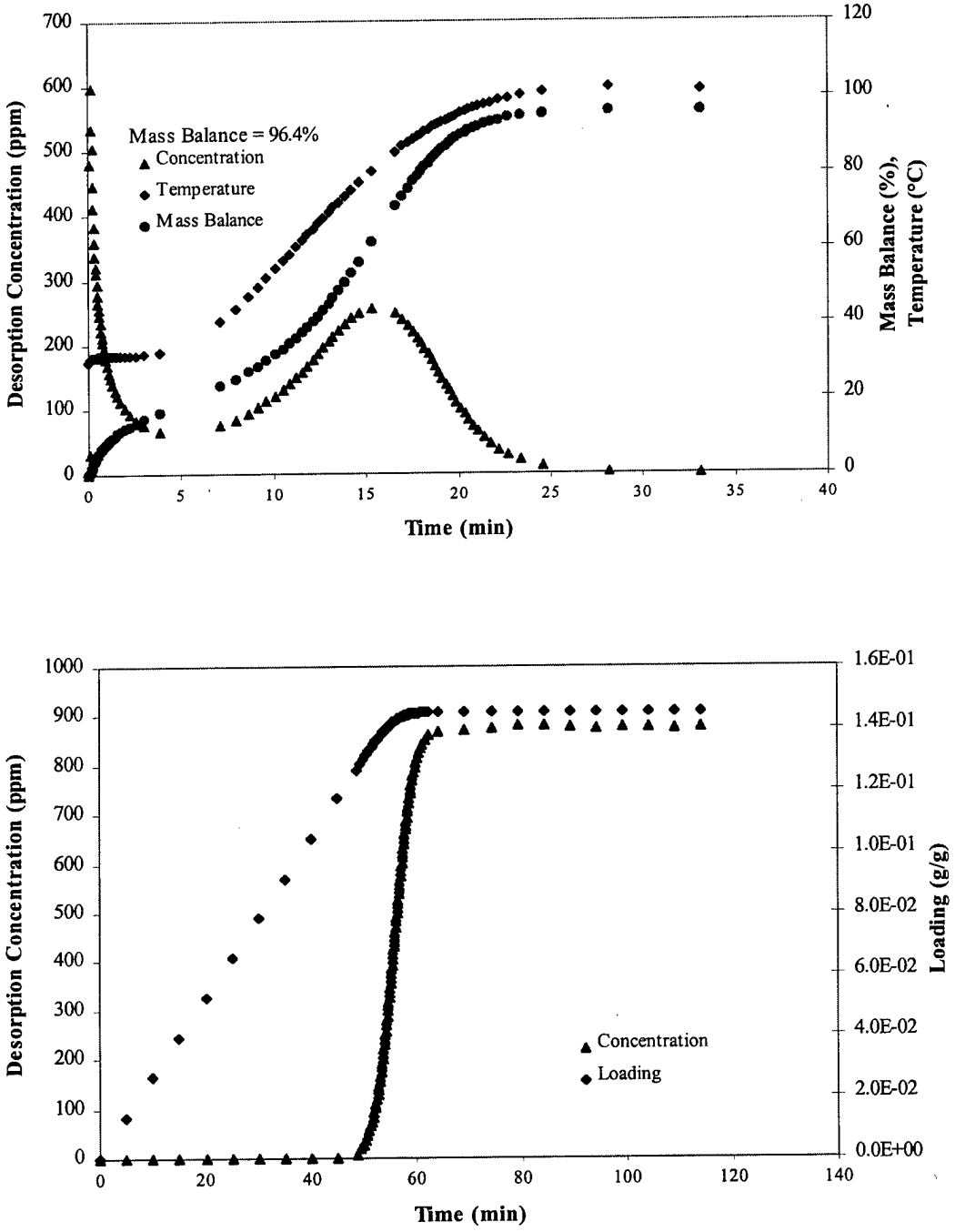

Figure A.26. Experiment No. 26 Results. Desorption (Top) and Breakthrough (Bottom) Results for Silica Gel 250Å with a 20,000 Ct Challenge.

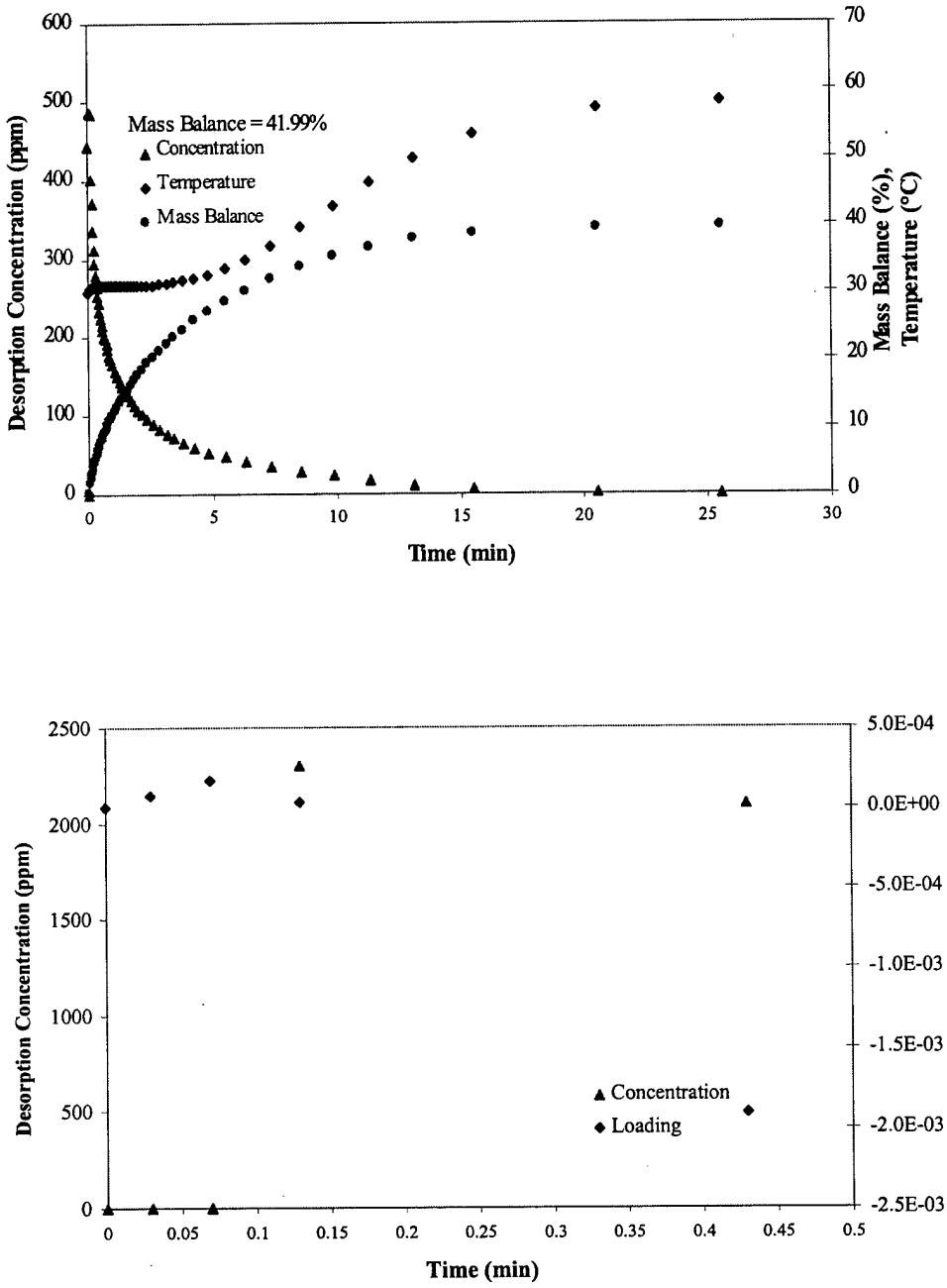

Figure A.27. Experiment No. 27 Results. Desorption (Top) and Breakthrough (Bottom) Results for Sorbead RF with a 20,000 Ct Challenge.

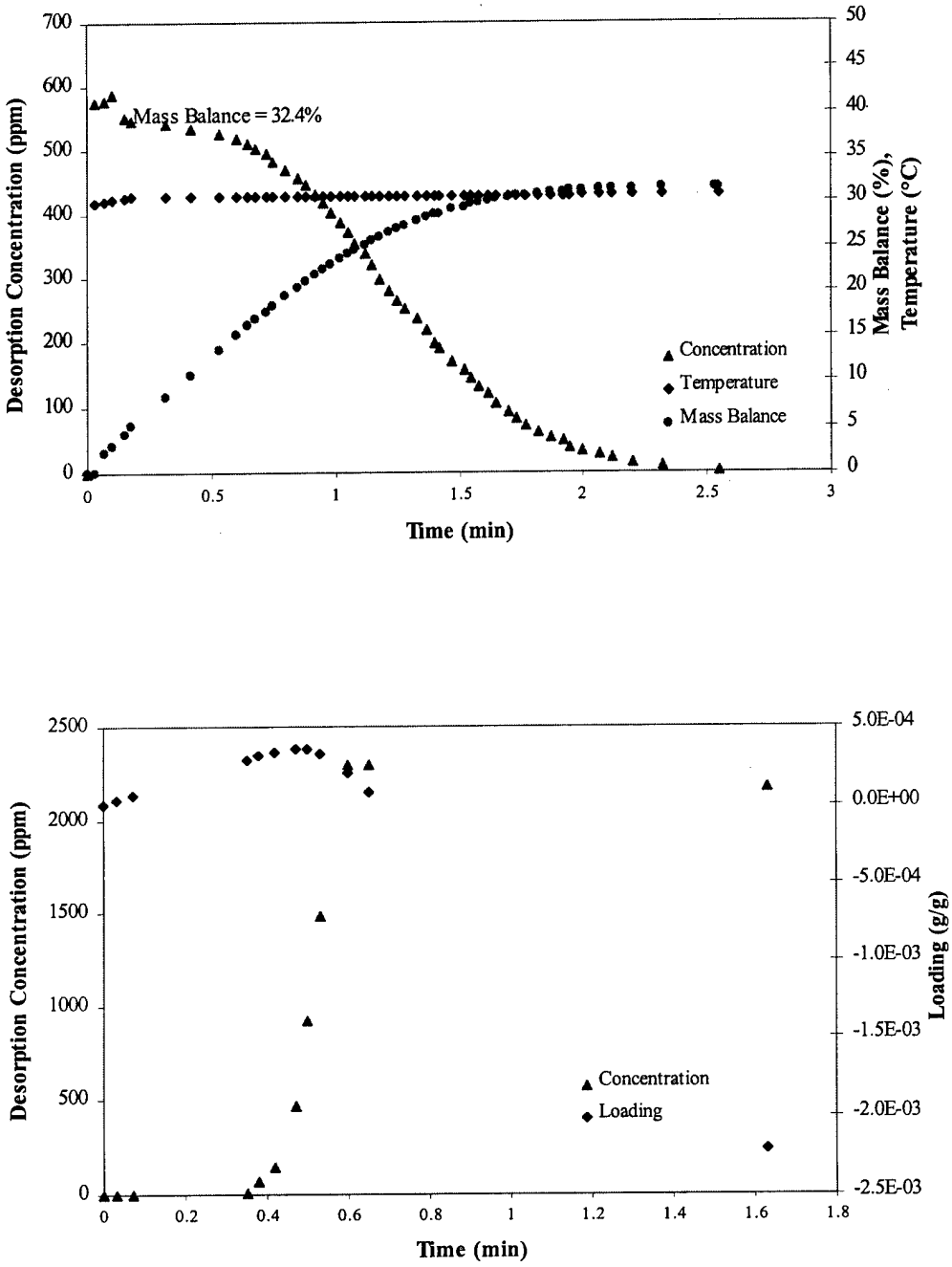

Figure A.28. Experiment No. 28 Results. Desorption (Top) and Breakthrough (Bottom) Results for Silica Gel 250Å with a 20,000 Ct Challenge.

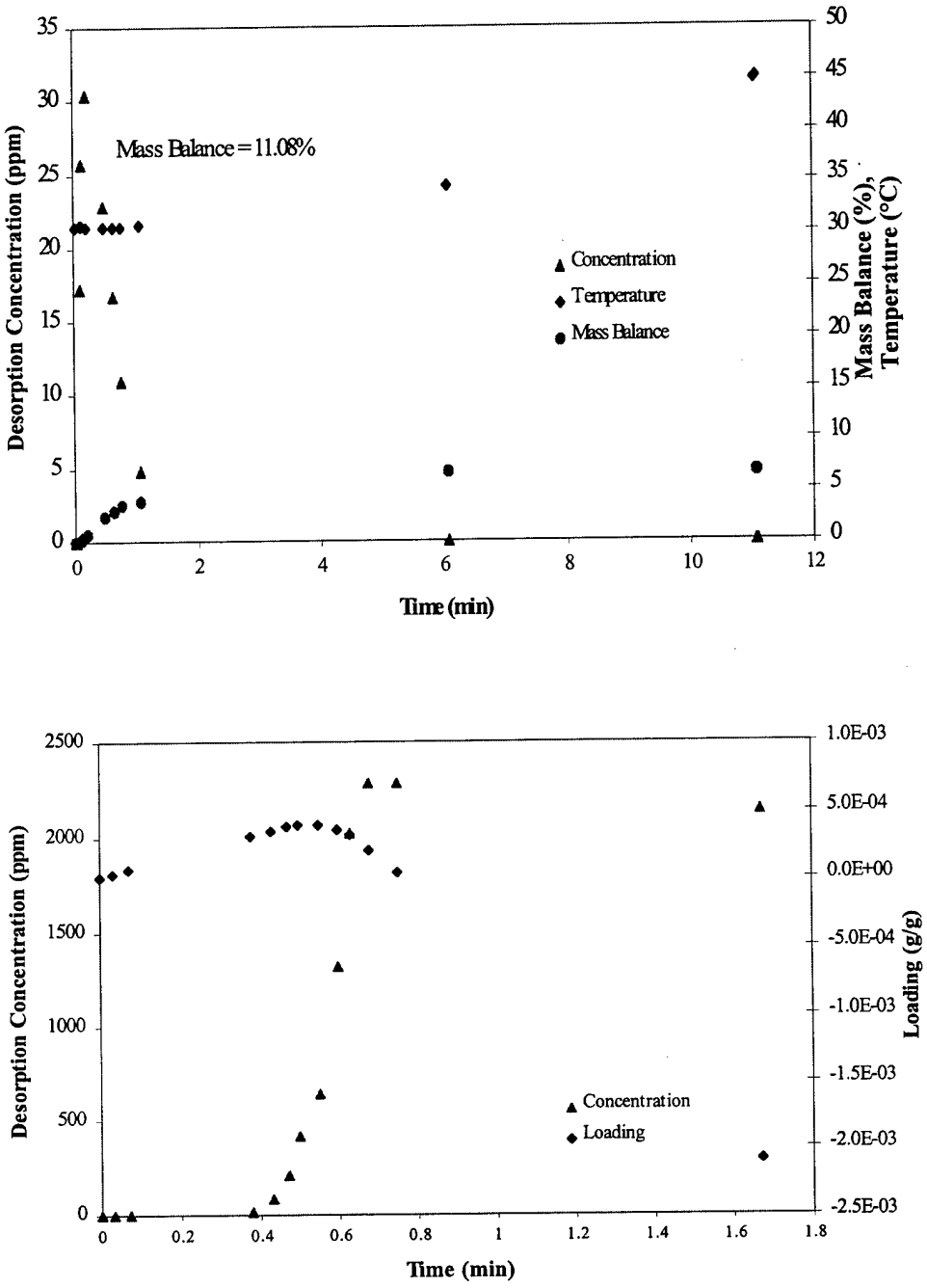

Figure A.29. Experiment No. 29 Results. Desorption (Top) and Breakthrough (Bottom) Results for Silica Gel 250Å with a 4,000 Ct Challenge.

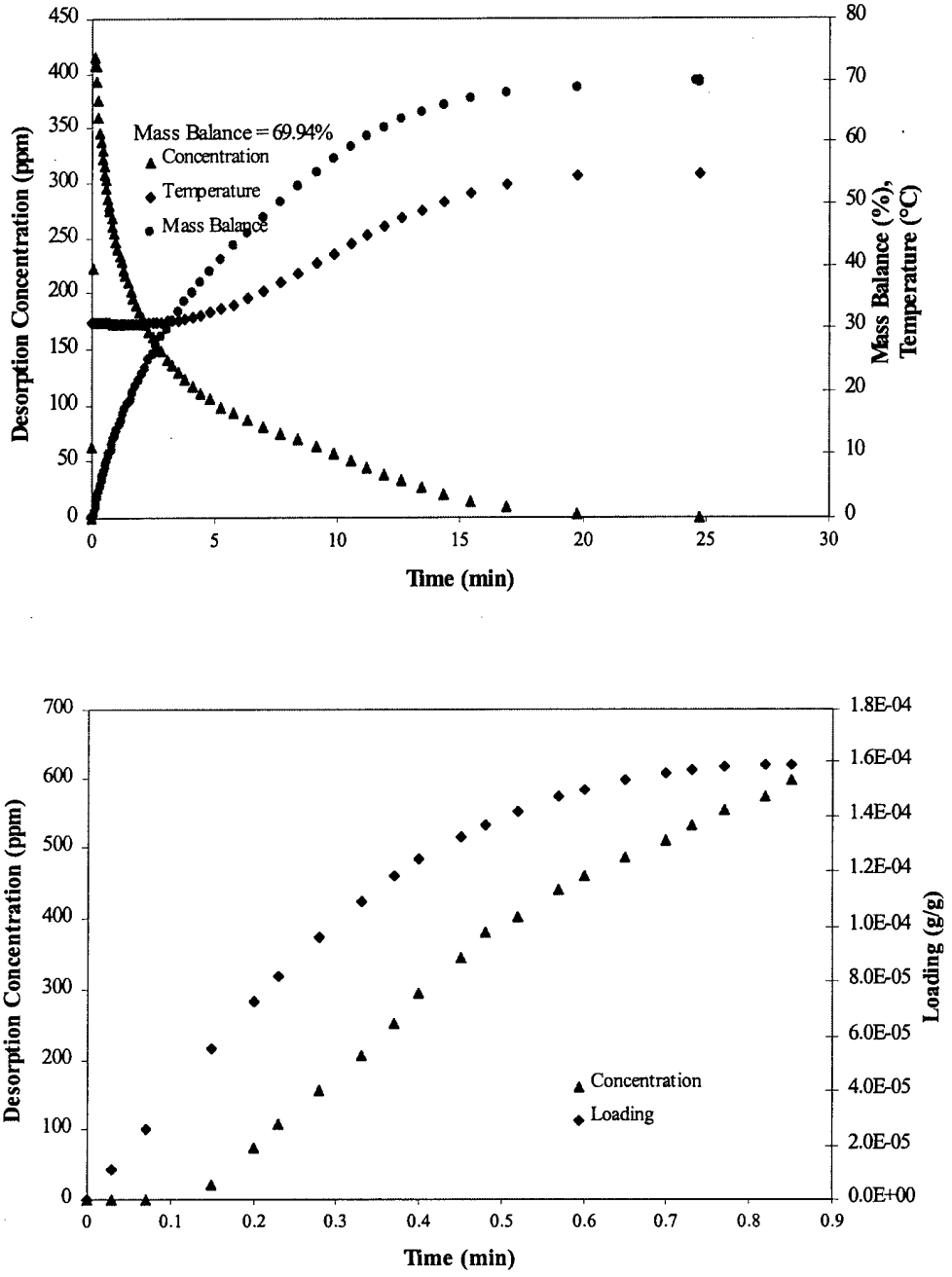

Figure A.30. Experiment No. 30 Results. Desorption (Top) and Breakthrough (Bottom) Results for Alumina with a 20,000 Ct Challenge.

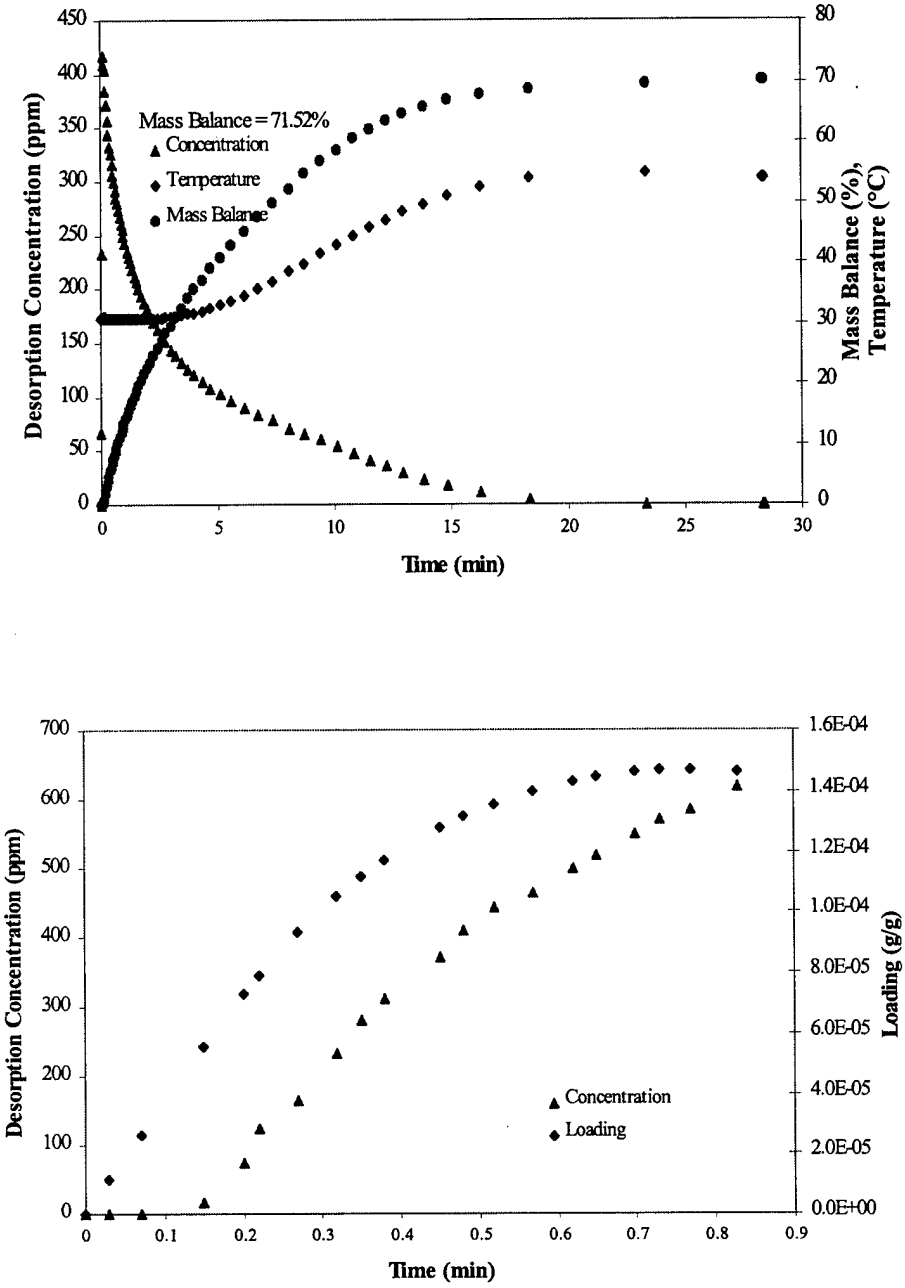

Figure A.31. Experiment No. 31 Results. Desorption (Top) and Breakthrough (Bottom) Results for Alumina with a 20,000 Ct Challenge.

Blank

APPENDIX B

DISCRETE SAMPLING AND SILICA GEL REGENERABILITY

Experiments discussed in the second half of this report are listed below in Table B. In addition, a plot of the results of each of the experiments listed in Table B are given.

Table B. Summary of Discrete Sampling and Silica Gel Regenerability Experiments.

Exp. No.	Date	Adsorbent	Adsorbate	Challenge Ct ($mg\text{-}min/m^3$)	Desorp.T (°C)	Mass Bal (%)
32	11/10/98	Alumina	2-Hexanol	7000	50	50
33	11/18/98	Silica Gel 40	2-hexanol	7000	50	133
34	11/20/98	Silica Gel 40	2-hexanol	7000	50	73
35	1/19/99	Silica Gel 500A	2-hexanol	7000	50	93
36	1/20/99	Silica Gel 500A	2-hexanol	7000	50	97
37	1/21/99	Silica Gel 500A	2-hexanol	7000	100	95
38	1/22/99	Silica Gel 70	2-hexanol	7000	50	91
39	1/25/99	Silica Gel 70	2-hexanol	7000	50	97
40	1/28/99	Silica Gel 40	2-hexanol	7000	50	90
41	2/1/99	Silica Gel 40	2-hexanol	7000	50	117
42	2/4/99	Silica Gel 250A	2-hexanol	7000	50	89
43	2/8/99	Silica Gel 250A	2-hexanol	7000	50	94

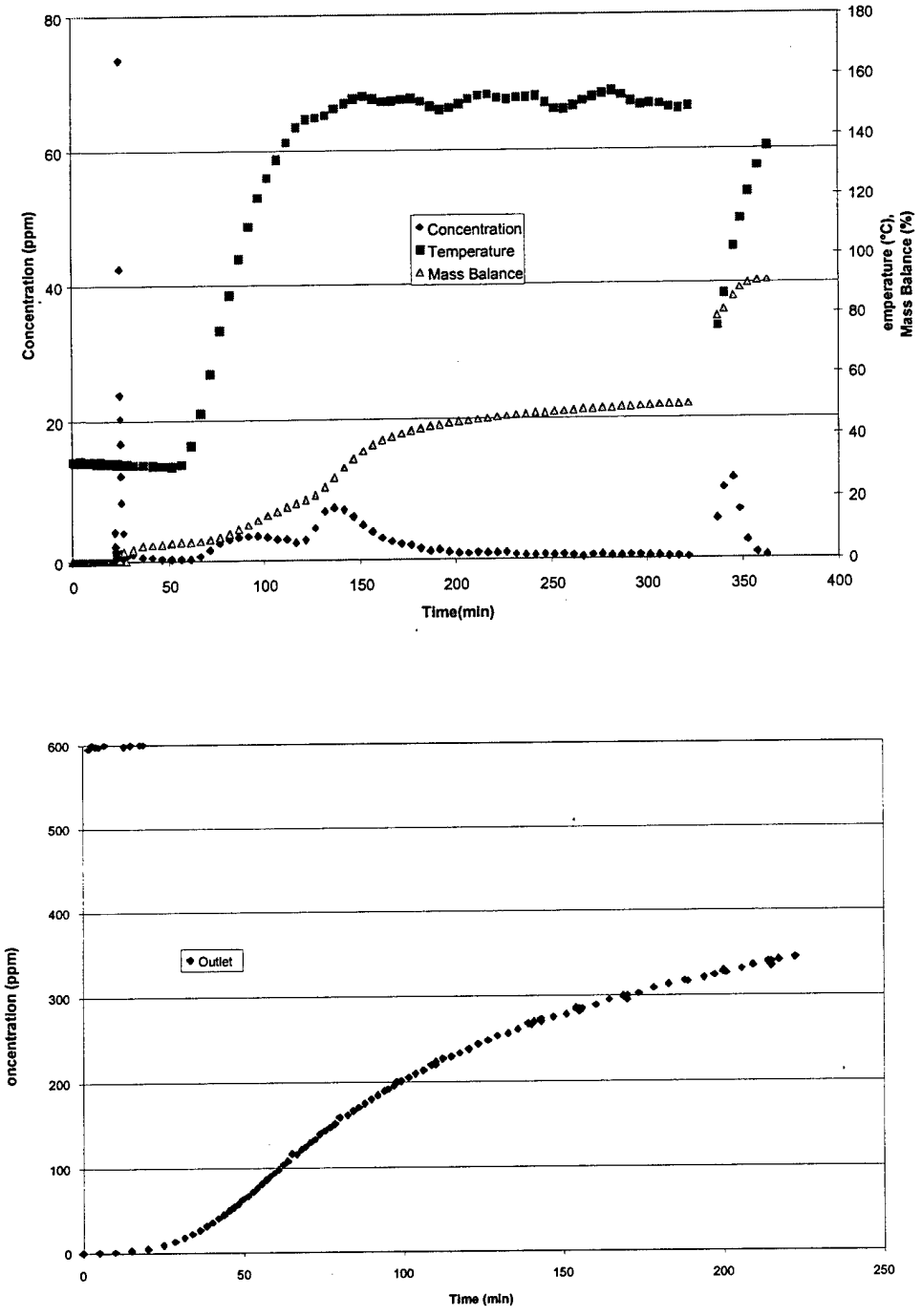

Figure B.1. Experiment No. 32 Results. Desorption (Top) and Breakthrough (Bottom) Results for Alumina with a 7,000 Ct Challenge.

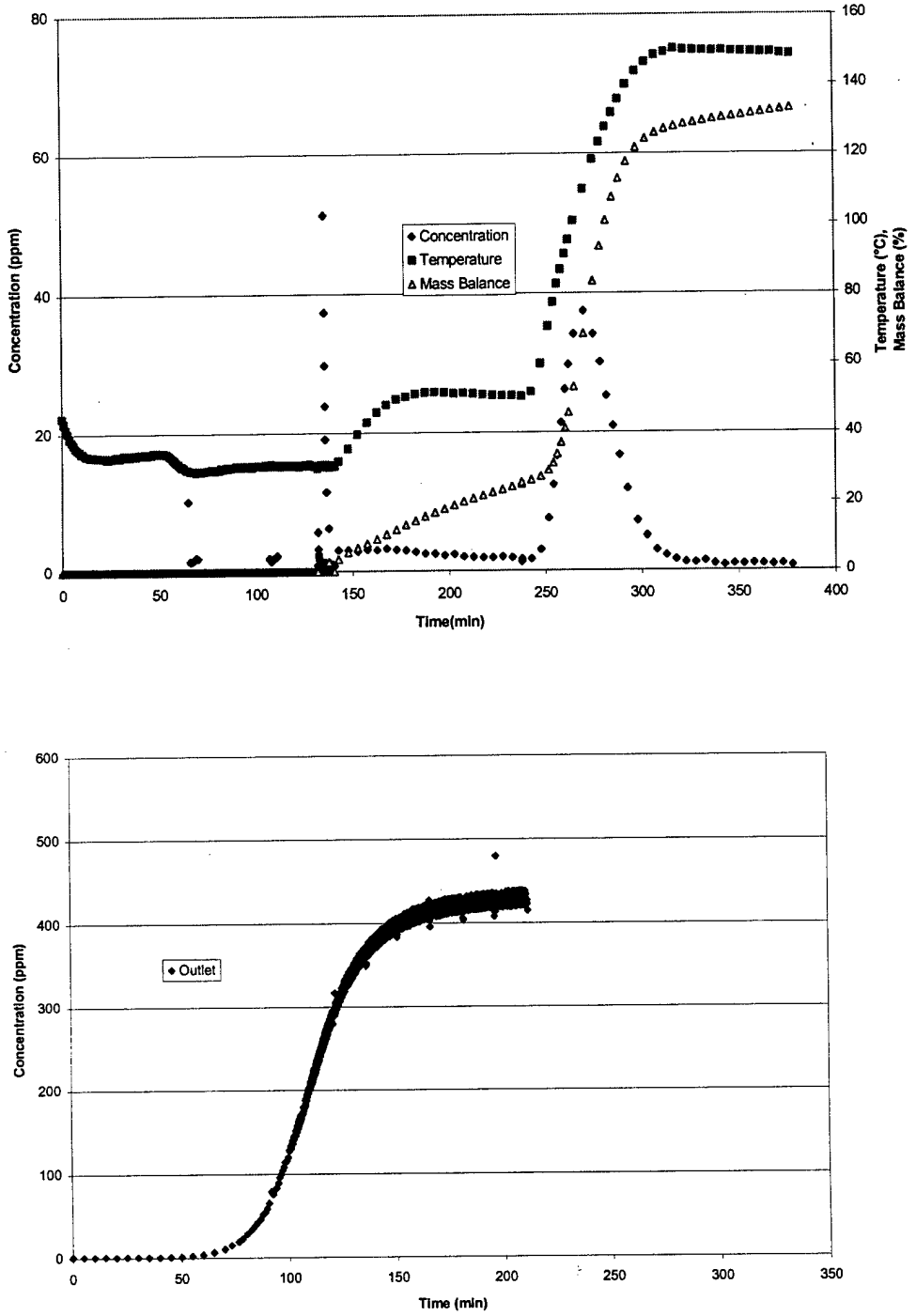

Figure B.2. Experiment No. 33 Results. Desorption (Top) and Breakthrough (Bottom) Results for Silica Gel 40 with a 7,000 Ct Challenge.

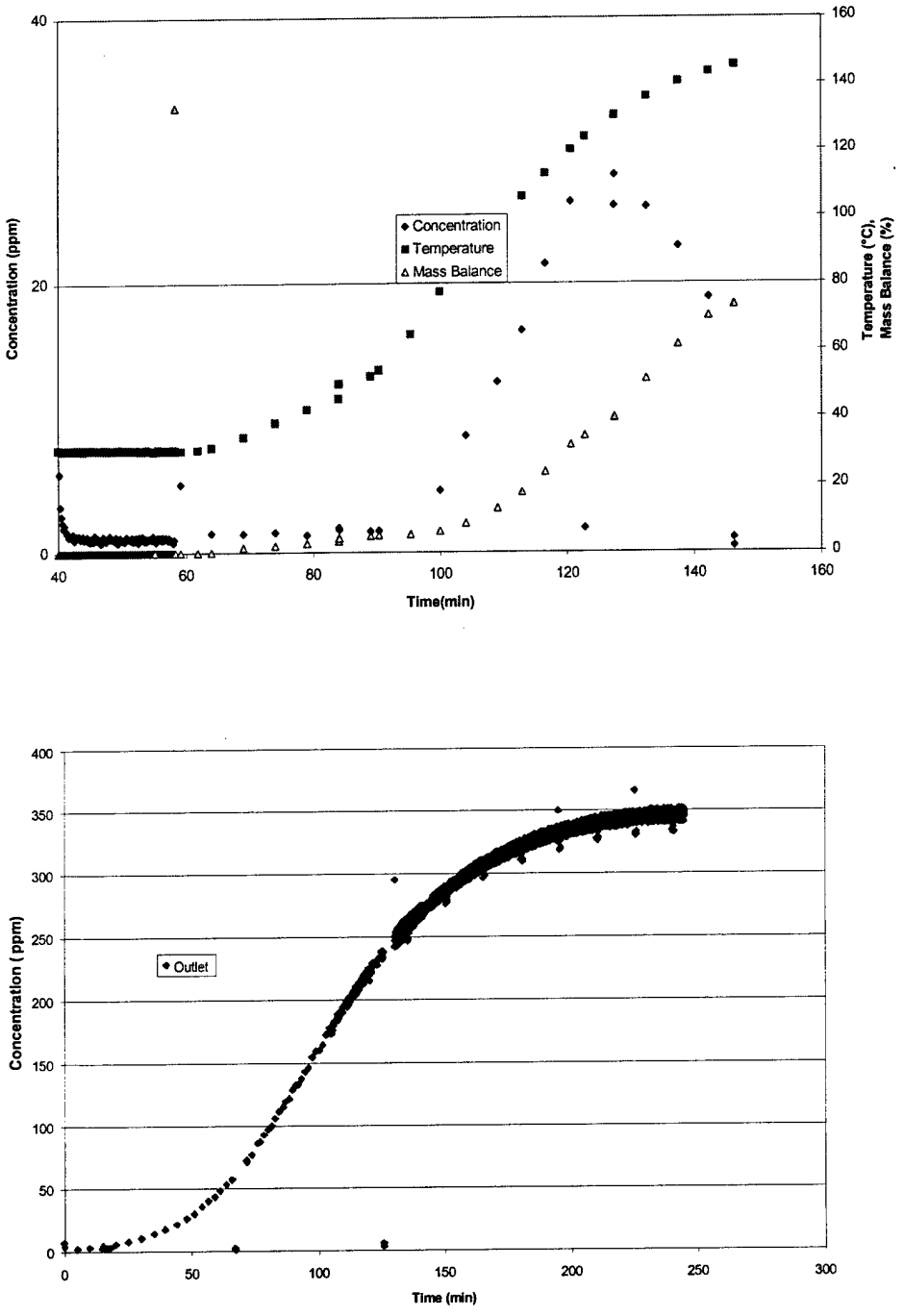

Figure B.3. Experiment No. 34 Results. Desorption (Top) and Breakthrough (Bottom) Results for Silica Gel 40 with a 7,000 Ct Challenge.

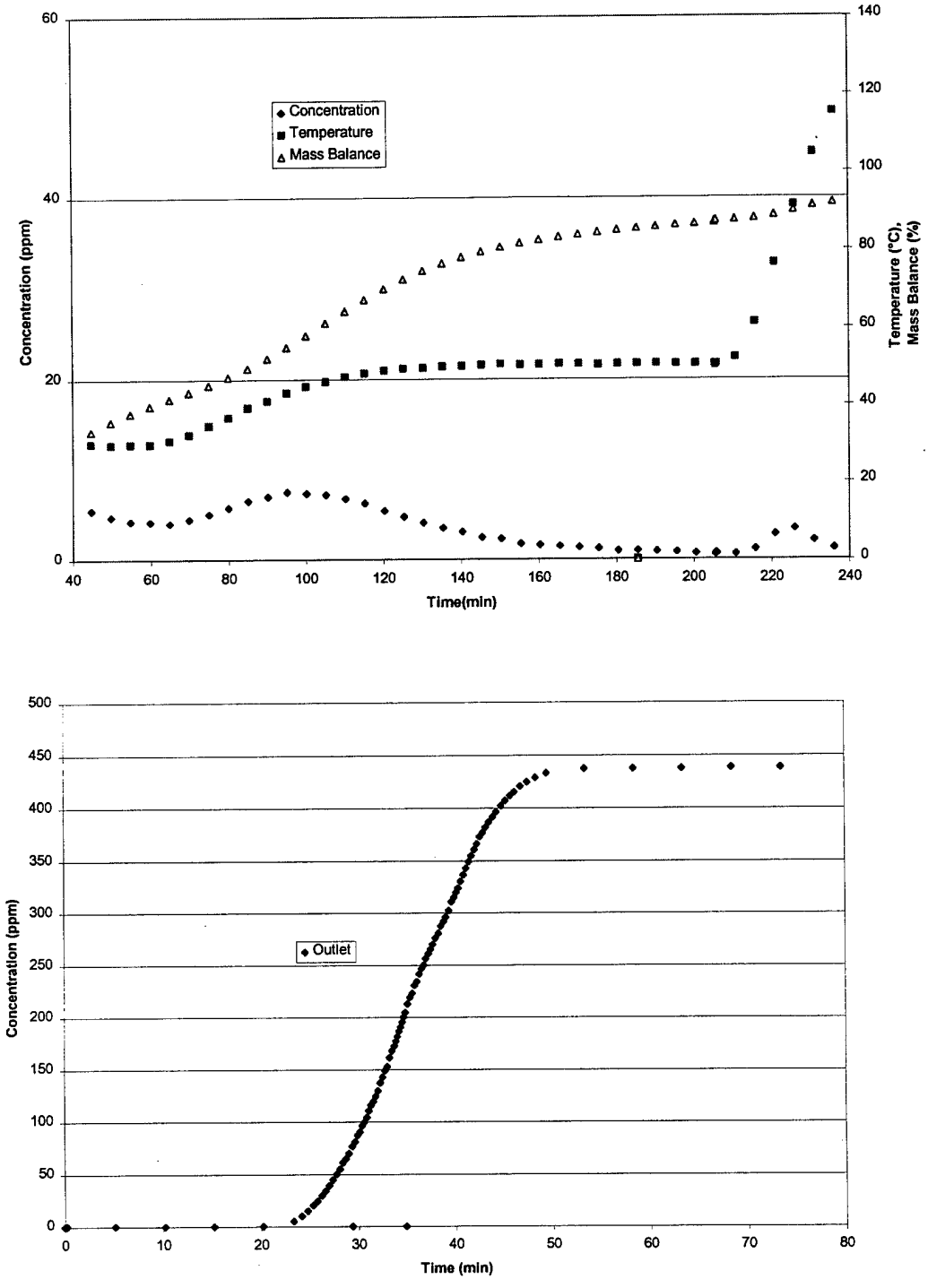

Figure B.4. Experiment No. 35 Results. Desorption (Top) and Breakthrough (Bottom) Results for Silica Gel 500A with a 7,000 Ct Challenge.

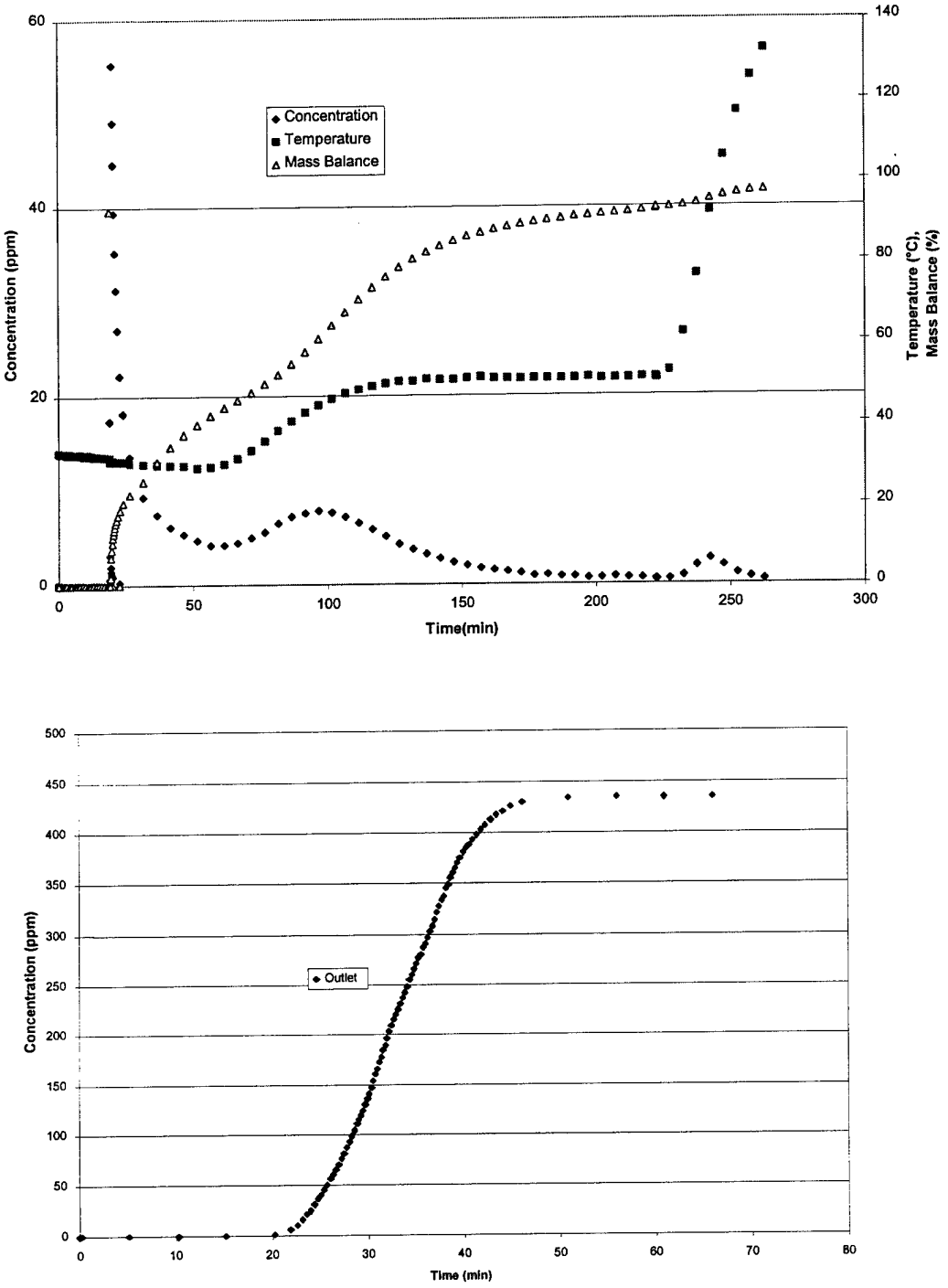

Figure B.5. Experiment No. 36 Results. Desorption (Top) and Breakthrough (Bottom) Results for Silica Gel 500A with a 7,000 Ct Challenge.

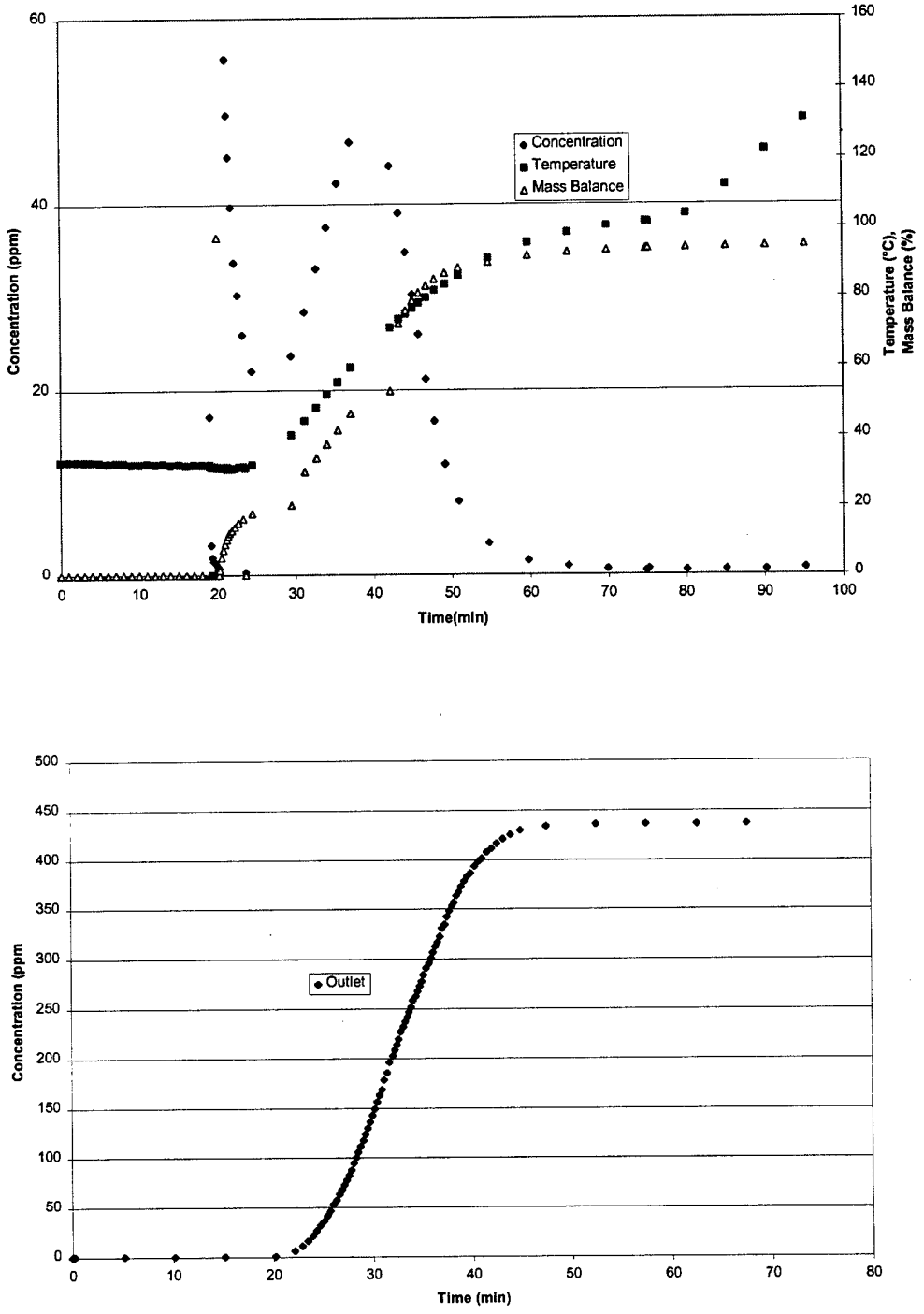

Figure B.6. Experiment No. 37 Results. Desorption (Top) and Breakthrough (Bottom) Results for Silica Gel 500A with a 7,000 Ct Challenge.

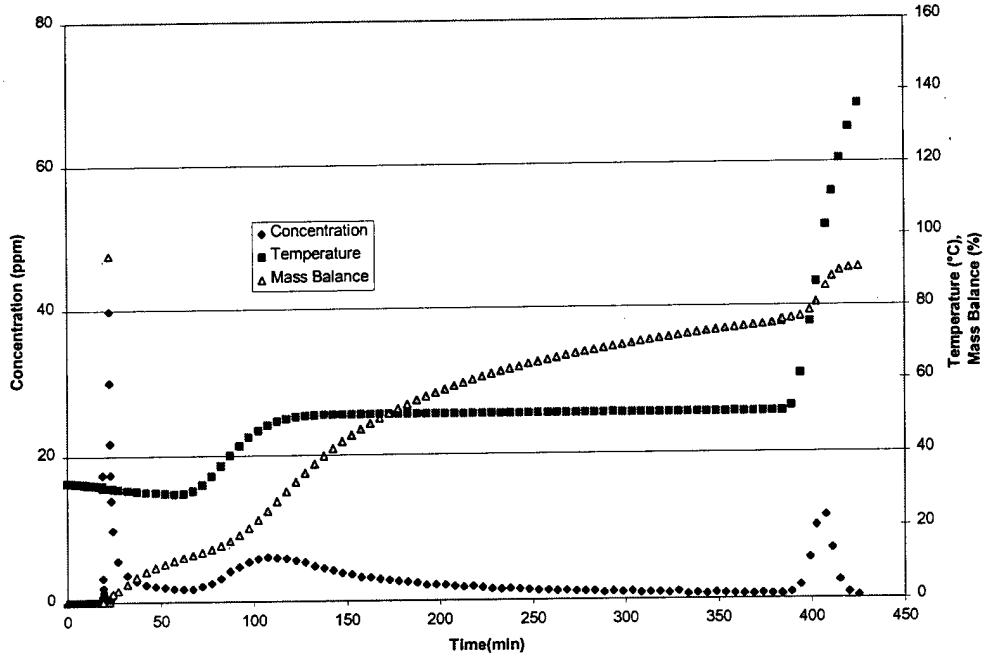

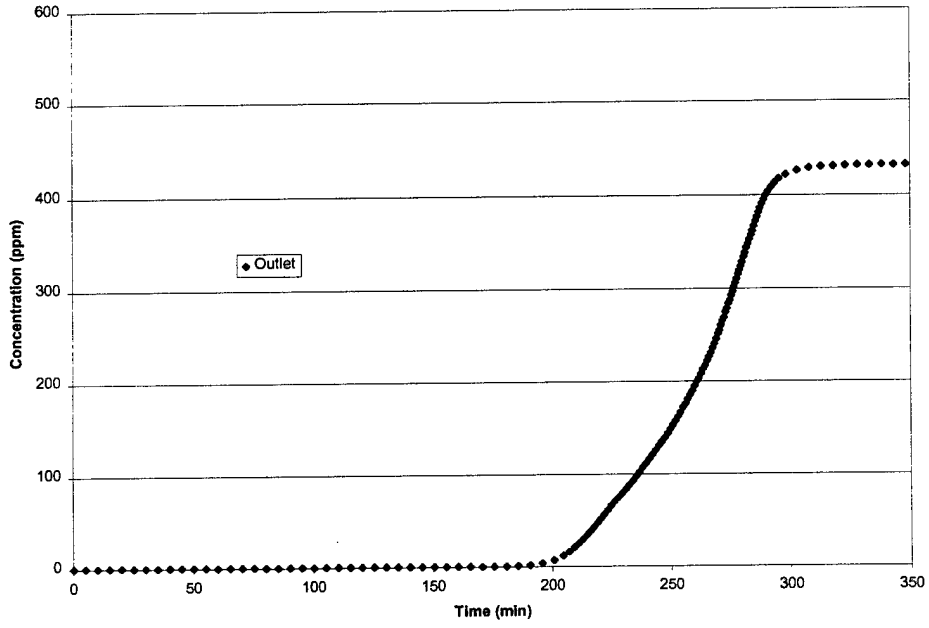

Figure B.7. Experiment No. 38 Results. Desorption (Top) and Breakthrough (Bottom) Results for Silica Gel 70 with a 7,000 Ct Challenge.

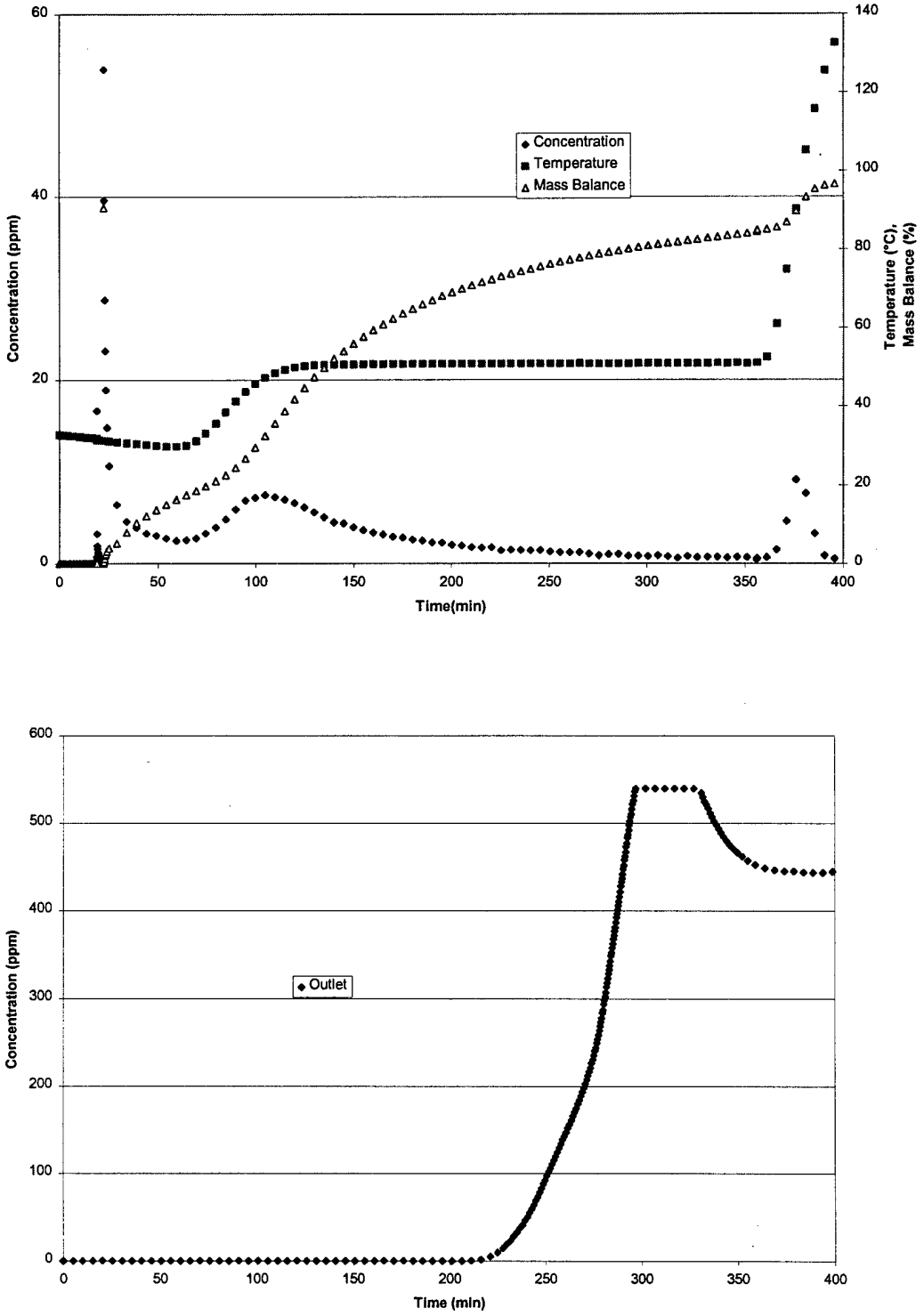

Figure B.8. Experiment No. 39 Results. Desorption (Top) and Breakthrough (Bottom) Results for Silica Gel 70 with a 7,000 Ct Challenge.

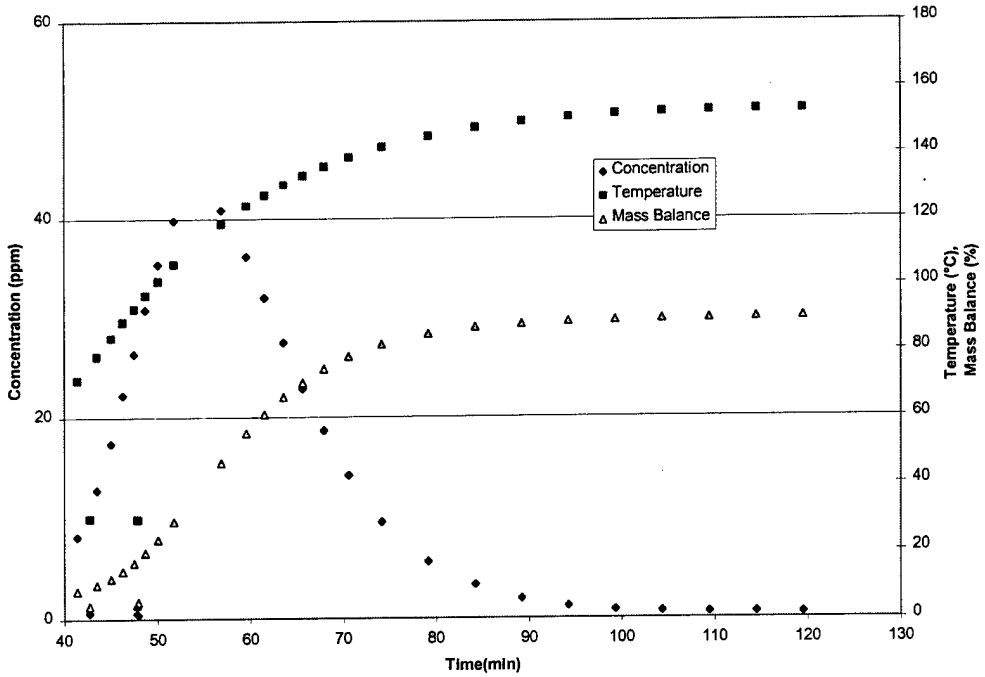

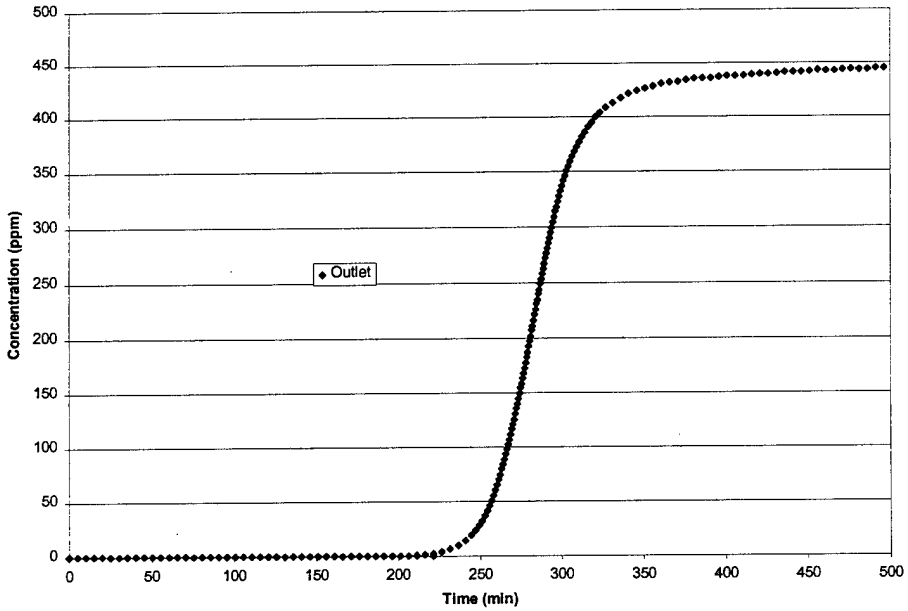

Figure B.9. Experiment No. 40 Results. Desorption (Top) and Breakthrough (Bottom) Results for Silica Gel 40 with a 7,000 Ct Challenge.

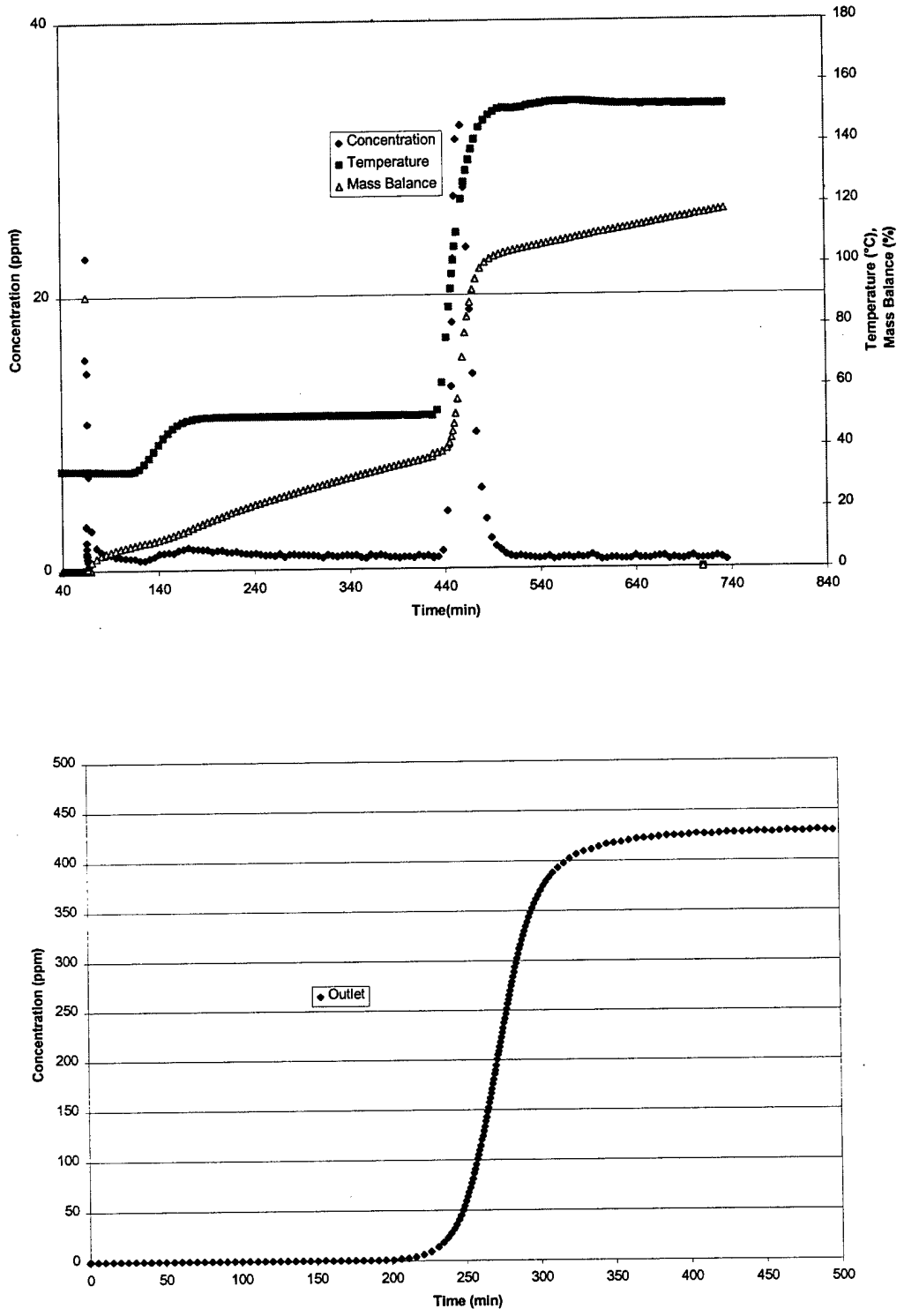

Figure B.10. Experiment No. 41 Results. Desorption (Top) and Breakthrough (Bottom) Results for Silica Gel 40 with a 7,000 Ct Challenge.

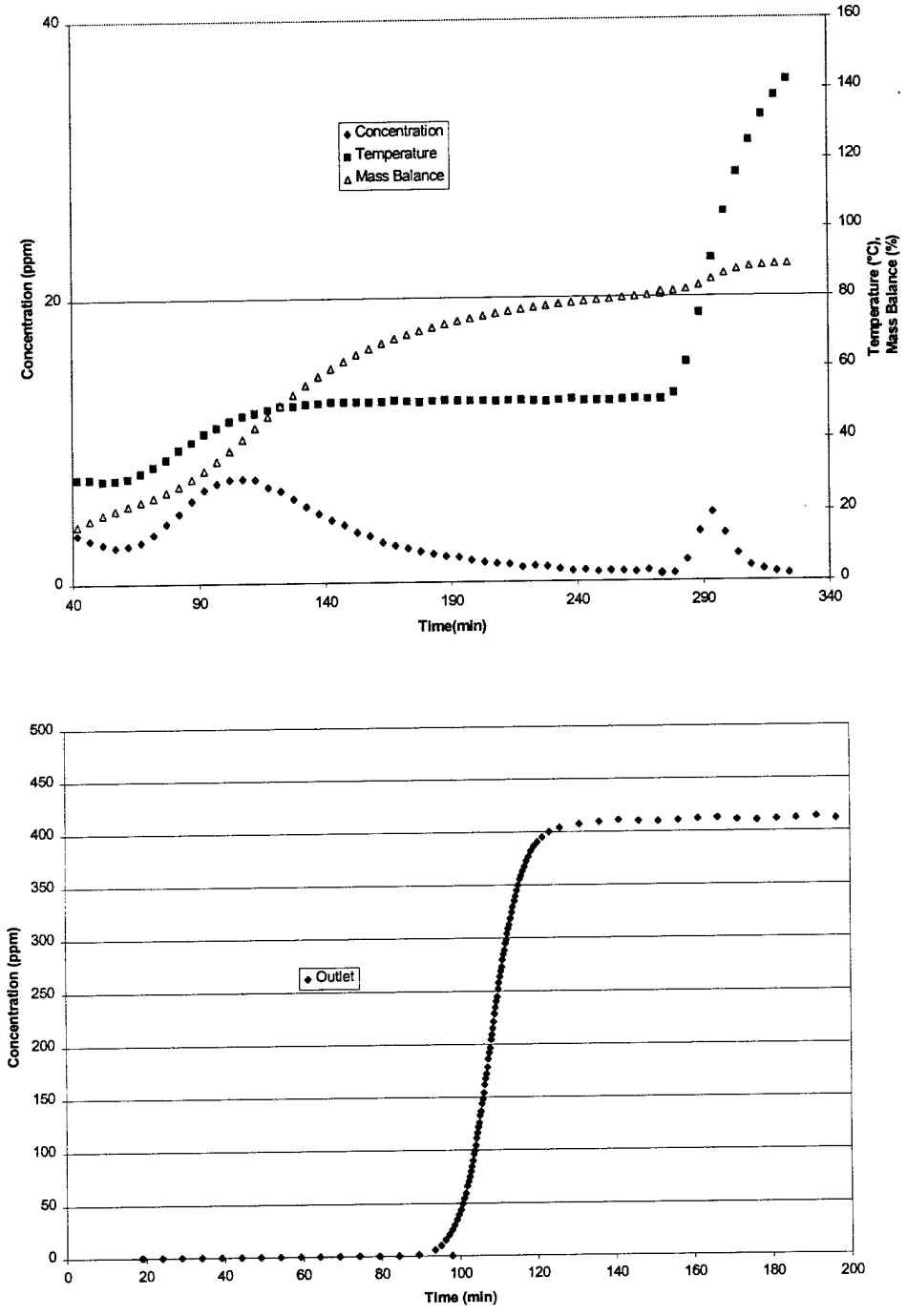

Figure B.11. Experiment No. 42 Results. Desorption (Top) and Breakthrough (Bottom) Results for Silica Gel 250A with a 7,000 Ct Challenge.

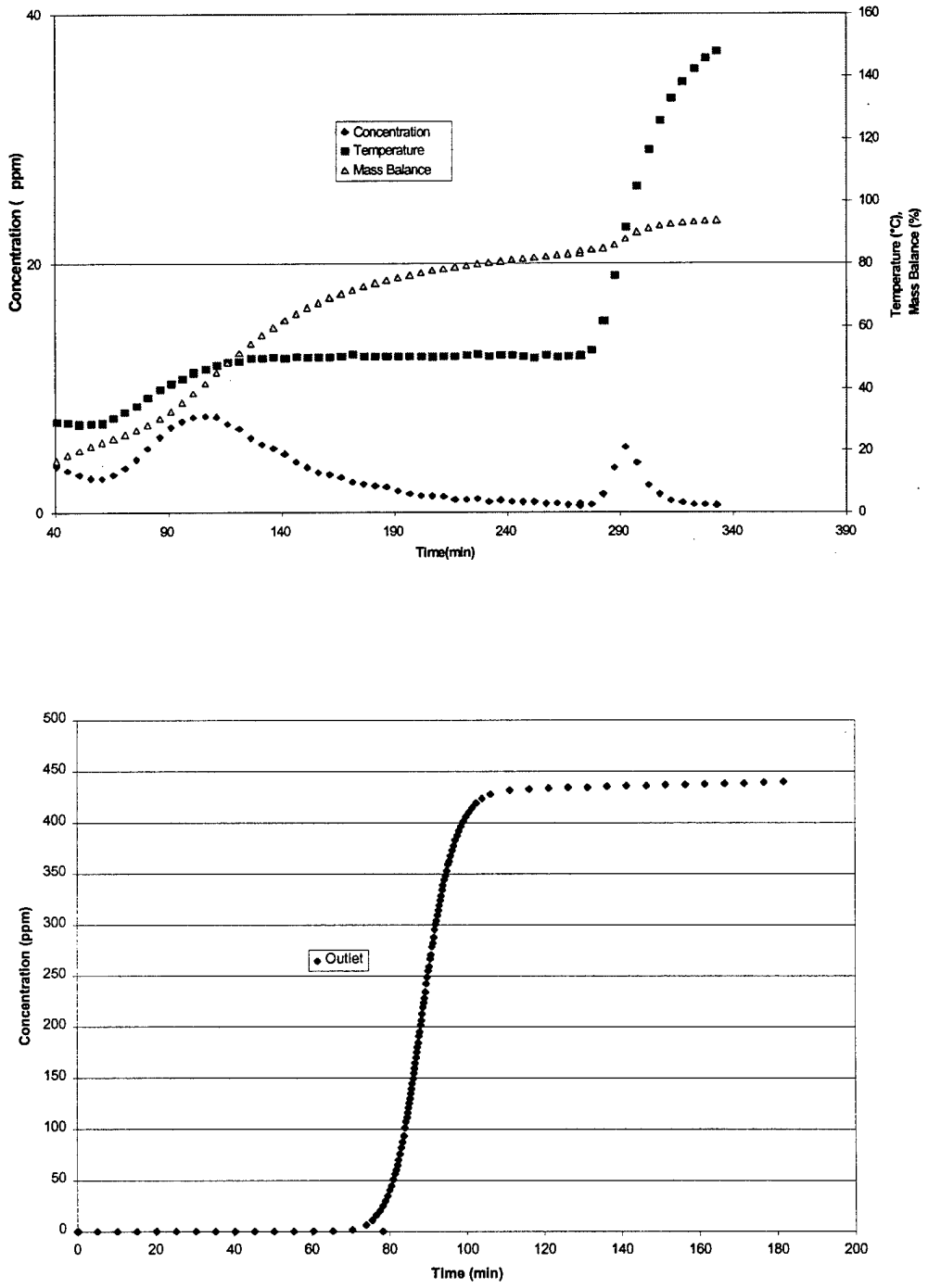

Figure B.12. Experiment No. 43 Results. Desorption (Top) and Breakthrough (Bottom) Results for Silica Gel 250A with a 7,000 Ct Challenge.